Chapter 4:

Evidence for the Buildup of the Thermobaric Capacitor in Deep North Atlantic Waters During the Last Deglaciation

4.1 INTRODUCTION

Ice core records from the past 800,000 years are broadly characterized by eight shifts from glacial to interglacial states forced by solar insolation on the 20,000, 40,000 and 100,000 year time scales (1). CO_2 and temperature closely follow each other during these shifts (Figure 4.1); however, there is a strong nonlinear response of climate to solar insolation. The classic "sawtooth" structure of glacial cycles requires an extra forcing, and although CO_2 rise does not precede glacial-interglacial (G/IG) shifts, it is one of the most important amplifiers to temperature change in the climate system. The deep ocean has been long been considered a central part of the climate shifts because it contains more than sixty times CO_2 than the atmosphere and is a large heat reservoir.

However, during the last glacial period, there were several extremely abrupt and large amplitude climate shifts characterized by dramatic changes in temperature (2). There are twenty one of these Dansgaard-Oeschger events and although they were first recognized in the ice cores, they have later been seen in a variety of marine (3, 4) and terrestrial archives (5, 6). Methane synchronization of the Greenland and Antarctic ice cores has shown that the Antarctica warms during the coldest of these rapid climate change events (Heinrich (H) Events) 1,000 to 3,000 years before Greenland (7). These changes further implicate the deep ocean as an important factor in climate shifts as the deep ocean is one of the only reservoirs in the climate system with the 'memory' to cause such a phase difference between Antarctica and Greenland on the millennial time scale.

The last termination or deglaciation is the most recent example of a G/IG climate shift. The termination began in Antarctica (8) and the Southern Ocean (9) at ~ 18 ka, and

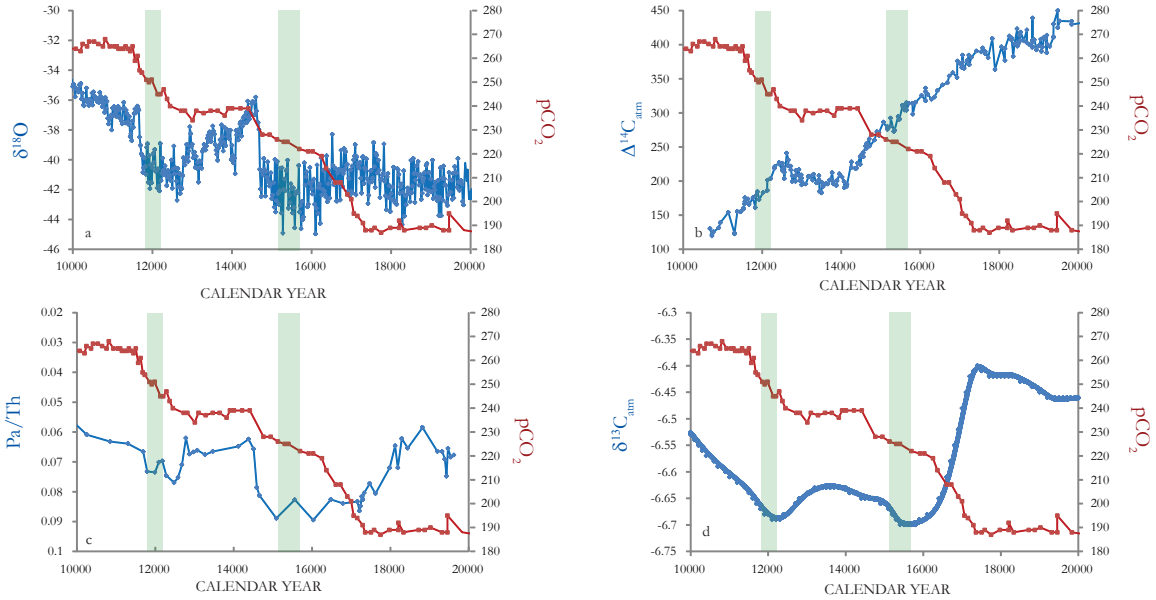

Figure 4.1: Ice core and marine recconstructions illustrating the evolution of major components of the climate system between 10 kya to 20kya. (A) pCO_2 and $\delta^{18}O$ (a proxy for temperature) reconstructions from ice core. (B) Reconstructed $\Delta^{14}C_{atm}$ from the ^{230}Th-dated Hulu cave record with pCO_2. (C) Pa/Th from the North Atlantic (a proxy for AMOC) with pCO_2. (D) $\delta^{13}C_{atm}$ of atmospheric CO_2 from the EPICA Dome C core and Talos Dome Ice Core with pCO2. All ice core records are plotted on a synchronized age scale. The grey shaded regions indicate the age range of corals used in the YD profile and H1 profile.

by 7,000 years only a small section of the Laurentide Ice Sheet that had covered all of North America was left. However, the warming was not gradual, but punctuated by several abrupt climatic shifts. Temperature records from Greenland and the North Atlantic reveal a cold interval (Heinrich Stadial 1) during which a massive ice rafted debris (IRD) field formed in the North Atlantic. This IRD event at 17.5 ka coincides with shut down of Atlantic Meridional Ocean Circulation (AMOC) circulation and the beginning of the rise in CO_2 (Figure 4.1c). In the North Atlantic, this cold interval was followed by an abrupt warming into the Bolling-Allerod (B/A) warm period at 14.7 ka. The B/A was then subsequently followed by a rapid return to near glacial conditions during the Younger Dryas (~ 12.8–11.5kya).

The Southern Hemisphere responded differently by warming more gradually between 17.5 ka and the Holocene. While Heinrich Stadial 1 (H1) in the Northern Hemisphere occurred, the Southern Hemisphere slowly warmed until the B/A. During the abrupt warming in the Northern Hemisphere, the Southern Hemisphere cooled (Antarctic Cold Reversal (ACR)) while CO_2 remained constant. As the Younger Dryas occurred in the Northern Hemisphere, the Southern Hemisphere slowly warmed and CO_2 began to rise.

To understand the role carbon cycle changes in these warmings, $\delta^{13}C_{atm}$ and $\Delta^{14}C_{atm}$ measurements have been made (Figure 4.1). These two carbon isotopes show some similar patterns to each other and CO_2 during the deglaciation. Both $\delta^{13}C_{atm}$ and $\Delta^{14}C_{atm}$ begin to decline at 17.5 ka. However there are extra features in these two records that are difficult to explain, for instance changes in slope at 16.2 ka and 15.4 ka that are difficult to explain.

There are two main hypotheses for explaining the offset between NH and SH. The first involves a southward shift to the Westerlies and the second is the "Bipolar See-Saw". Chiang and Bitz (10) demonstrated that the spread of winter sea ice over the Northern North Atlantic shifts the ITCZ and Southern westerly wind belt further south. This mechanism rapidly transfers the climate signal between hemispheres.

The Bipolar See-Saw is a marine-based explanation and involves an oscillating

AMOC regime hypothesized to be driven by changes in North Atlantic Deep Water (NADW) and Antarctic Bottom Water (AABW) formation. It is instigated by an increase in Northern Hemisphere summer insolation, which melts ice to trigger a reduction in AMOC. This reduction cools the Northern Hemisphere at the expense of warming the Southern Hemisphere. Eventually CO_2 is degassed from a warm, radiocarbon depleted and carbon rich water mass in the Southern Ocean, triggering global warming and the resumption of the AMOC. It is possible the two mechanisms occurred together with the bipolar see saw helping move the zonal wind systems further South by changing the sea surface temperature gradients (11).

The exact mechanism for the resumption of the AMOC after the release of CO_2 is not known, but one explanation for the resumption which is also consistent with the patterns of warming seen in the different hemispheres is the "Thermobaric Capacitor" hypothesis" (12). Pore fluid estimates of the distribution of $\delta^{18}O_w$ during the Last Glacial Maximum (LGM) shows that modern arrangement of salty northern source waters and relatively fresh southern source waters was reversed during the Last Glacial Maximum (LGM) and that salt dominated the stratification of the deep Atlantic (13). The "Thermobaric Capacior" hypothesis proposes that in the presence of a salt stratified deep ocean, geothermal heat (or warm deep isopycnals) can warm the deepest layers of the ocean while maintaining the static stability of the water column. The thermobaricity of seawater can allow for a virtually instantaneous release of the energy stored in the warm deep water causing abrupt overturning of the water column. This overturning can bring salt to the areas of deep-water convection in the glacial North Atlantic and reinvigorate northern source deep-water formation.

In Chapter 2 we have demonstrated that clumped isotope paleothermometry can be used to generate subdegree precision temperature reconstructions. In Chapter 3 we radiocarbon dated several hundred fossil deep-sea corals to determine their spatial and temporal range. In this study we utilize the results of the previous two chapters. Here, we

present radiocarbon and temperature profiles during the Younger Dryas (YD) and Heinrich 1 (H1) that provide new insights into the role of the ocean in deglacial releases of CO_2 and support for the thermobaric capacitor hypothesis.

4.2 METHODS

Samples examined in this study were obtained from the Caltech Deep-Sea Coral Fossil Collection. The deep-sea corals were *Desmophyllum dianthus* from the New England (34−40°N, 60−68°W) and Corner Rise Seamounts (34−36°N, 47−53°W) collected in 2003−2005 using the deep submergence vehicles ALVIN and HERCULES. Collection by ROV and submarine ensured that the depth of each coral was precisely known and that corals were collected near growth position. All samples in this study were analyzed for U/Th ages, ^{14}C ages and Δ_{47} temperatures.

4.2.i Radiocarbon Dating Method

All samples analyzed for ^{14}C and U/Th were physically cleaned with a Dremel tool, and chemically cleaned by ultrasonicating alternately in $NaOH/H_2O_2$ and MILLI Q water, and then rinsed with Methanol and leached in $HClO_4/H_2O_2$ (14). After this step, an aliquot of 1g was removed for U/Th analysis. Twenty mg of coral was then taken to UC-Irvine for radiocarbon analysis. There, immediately prior to phosphoric acid dissolution and graphitization, each sample was leached in HCl to remove, typically, 50% of its total mass. The resulting coral was hydrolyzed in phosphoric acid, and the evolved CO_2 was graphitized under H_2 on an iron catalyst for ^{14}C analysis (14). Radiocarbon ages were measured at the UC-Irvine Keck-CCAMS facility on an Accelerator Mass Spectrometer.

4.2.ii U-Series Methods

Remaining aliquots of 1 g of coral were processed to extract U and Th (15). Corals were dissolved in concentrated SEASTAR nitric acid and spiked with a ^{229}Th-^{236}U double spike. Uranium and Thorium were scavenged from the resulting solution by iron precipitation. The iron pellet was then dissolved in 8N SEASTAR nitric acid. Uranium and Thorium fractions were separated using trace metal-clean Teflon columns and a Bio

Rad AG-1X-8 Cation Exchange Resin. Eluted fractions were dried down several times after successive drop wise additions of concentrated perchloric acid and SEASTAR nitric acid.

Uranium and Th fractions were brought up in 5% SEASTAR Nitric Acid and separately run on a multi collector inductively coupled mass spectrometer. All samples were bracketed by an instrumental standard or SGS to correct for mass bias and mass drift. Calculated $\delta^{234}U_{initial}$ values ranged from 144–155‰.

4.2.iii Δ_{47} Analysis

All coral samples were physically cleaned with a Dremel tool. Fossil corals, unlike modern corals, typically have a Fe-Mn crust surrounding them. This crust contains trapped organic matter, and can skew isotopic measurements of the bulk coral. A cleaning study was performed on a modern coral and a coral with Fe-Mn crust from Tasmania that had the same radiocarbon age as the modern ocean from which it was collected (Figure 4.2) to determine the best method for removing the Fe-Mn crust. Corals were cleaned four different ways. The first was only physical cleaning with a Dremel tool, the second was physical cleaning and chemical cleaning with 1:1 H_2O_2:NaOH, the third was physical cleaning, and chemical cleaning with 1:1 H_2O_2:NaOH and MeOH and the fourth was physical cleaning and chemical cleaning with 1:1 H_2O_2:NaOH , MeOH and $HClO_4$. It was determined that physical cleaning with a Dremel tool was the only method that yielded expected temperatures.

All fossil corals were cleaned according to procedures detailed in Chapter 2. Corals were physically cleaned with a Dremel tool and powdered with a mortar and pestle. Samples were dissolved in 105% H_3PO_4 at 90°C. The evolved CO_2 was analyzed in a Dual Inlet Finnigan MAT-253 mass spectrometer with the simultaneous collection of ion beams corresponding to masses 44–49 to obtain Δ_{47}, Δ_{48}, Δ_{49}, $\delta^{13}C$ and $\delta^{18}O$ values. The mass 47 beam is composed of $^{17}O^{13}C^{17}O$, $^{17}O^{12}C^{18}O$ and predominantly $^{18}O^{13}C^{16}O$ and we define R^{47} as the abundance of mass 47 isotopologues divided by the mass 44 isotopologue. ($R^{47}=[^{17}O^{13}C^{17}O+ {}^{17}O^{12}C^{18}O+{}^{18}O^{13}C^{16}O\ ]/[\ {}^{16}O^{12}C^{16}O]$.) Δ_{47} is reported

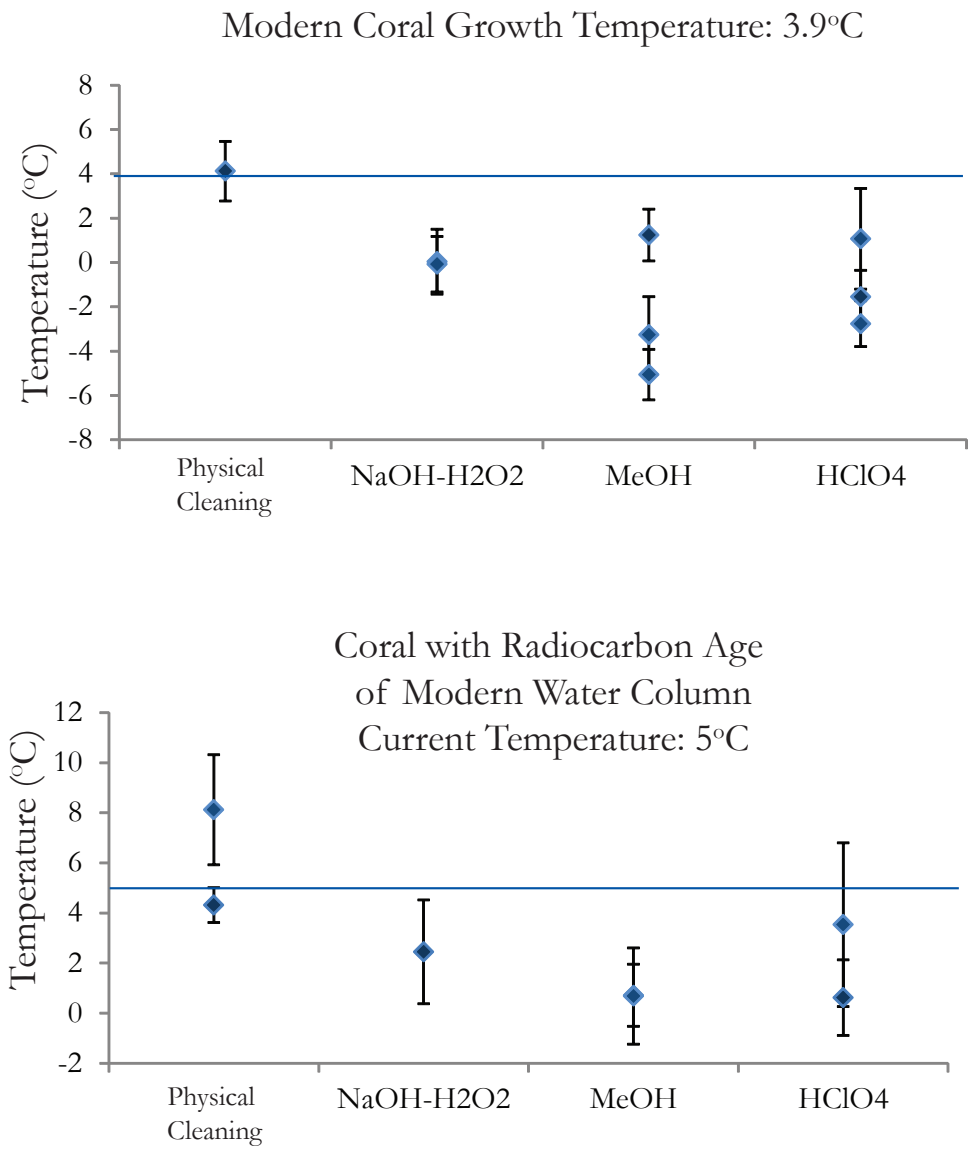

Figure 4.2: Cleaning experiment conducted to determine the best method to remove Fe-Mn crust from fossil corals. A modern coral was cleaned with the cleaning regimen used for radiocarbon cleaning. Reaction with the solvents likely dissolved the carbonate and changed the clumped isotope ratio. A fossil coral with the same age as the water column was also cleaned using the same protocol, and again the cleaning procedure did remove the Fe-Mn crust but also changed the clumped isotope ratio. For all subsequent clumped isotope analyses, corals were only physically cleaned.

relative to a stochastic distribution of isotopologues for the same bulk isotopic composition. (Δ_{47}=(((R$^{47}_{measured}$/R$^{47}_{stochastic}$)-1)- ((R$^{46}_{measured}$/R$^{46}_{stochastic}$)-1)- ((R$^{45}_{measured}$/R$^{45}_{stochastic}$)-1))*1000.) Mass 48 was monitored to detect any hydrocarbon contamination. Measurements of each gas were done at 16V of mass 44 and consisted of 8 acquisitions, each of which involved 7 cycles of sample-standard comparison with an ion integration time of 26s per cycle. Internal standard errors of this population of acquisition to acquisition for Δ_{47} ranged from 0.005–0.01$^{o}/_{oo}$, (1–2^{o}C) while external standard error ranged from 0.005–0.011 $^{o}/_{oo}$ (0.5–2^{o}C). The internal standard error for δ^{13}C ranged from 0.5-80ppm and the internal standard error for δ^{18}O ranged from .9–36ppm. Samples were corrected to standards run during the same session

4.3 RESULTS

We have examined 15 corals for U/Th ages, ^{14}C ages and Δ_{47} temperatures (Table 4.1, Table 4.2, Table 4.3, Table 4.4, Table 4.5, Table 4.6 and Table 4.7, and Figure 4.3). We selected these corals based on the results of a reconnaissance age screening dataset (16) made at NOSAMS at WHOI using a zinc-combustion method (17). These corals were then selected for high-precision ^{14}C dating and clumped isotopologue CO_2 measurements, and U/Th dating. The U/Th dating revealed that five of the analyzed corals were dated to the YD (11.7–12.1 ka BP), one was dated to the Bolling Allerod Event (13.8 ka), six corals were dated to late H1 (15.1–15.7 ka BP, and three corals were dated to early H1 /early deglaciation (16.1–17.7 ka BP). One of the H1 corals, NT 031, has an elevated $^{234}U_i$, so is not included in the Δ^{14}C profiles. These corals are not all at the same YD and H1 calendar age as the reconnaissance dating method had implied because the reconnaissance dating method has larger error bars than U/Th dating. Figure 4.3 shows the Δ_{47} reconstructed temperature profile and the Δ^{14}C profile for the Younger Dryas and Heinrich 1.

During the course of making clumped isotope measurements, we found that there is a possible vital effect in some deep-sea corals (Table 4.4 and Figure 4.4). Measurements with

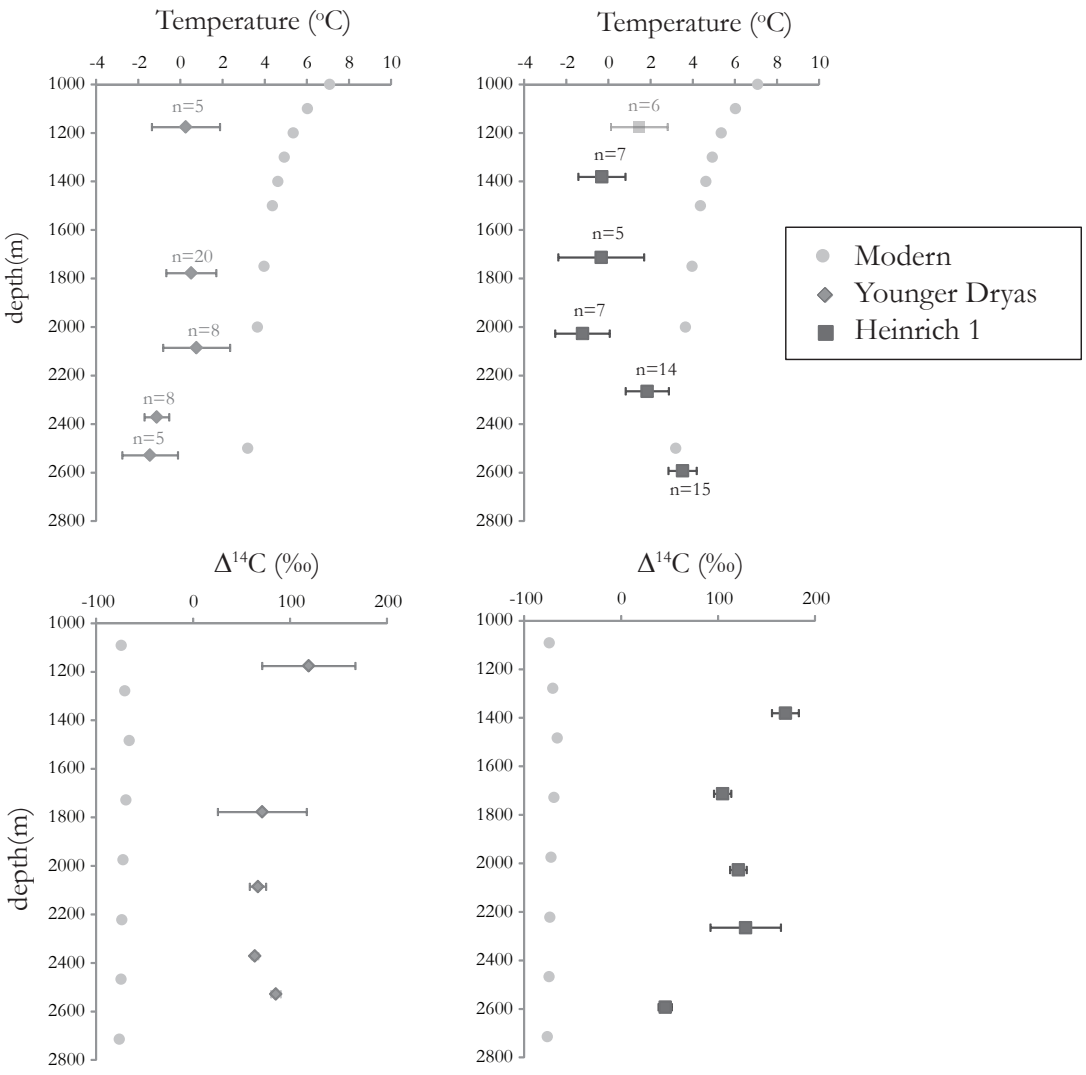

Figure 4.3: The temperature profiles for both the YD and late H1 are cooler than modern. The YD profile is isothermal at all measured depths while the H1 profile exhibits slight warming with depth. The $\Delta^{14}C$ profile for the YD is nearly constant with depth, while the H1 profile shows a depleted point at ~ 2600 m.

Table 4.1-Names and depths of Corals Analyzed

		sample name	seamount	depth
NT	001	ALV-3891-1646-004-001	GREGG	1180
NT	002	RBDASS05-H11-0826-0029-201-4-006-2529	NASHVILLE	2529
NT	006	RBDASS05-H03-0815-1004-314-3-002-1427	LYMAN	1427
NT	007	ALV-3885-1239-001-010	MUIR	2026
NT	009	ALV-3887-1549-004-007	MUIR	2372
NT	010	ALV-3887-1549-004-009	MUIR	2372
NT	011	ALV-3885-1239-001-004	MUIR	2027
NT	012	ALV-3892-1315-001-008	MANNING	1713
NT	013	ALV-3887-1652-005-013	MUIR	2265
NT	014	ALV-3890-1330-002-007	MANNING	1886
NT	015	RBDASS05-H15-0831-2045-605-020-2459	KELVIN	2529
NT	016	RBDASS05-H15-0831-1616-601-3-003-2593	KELVIN	2593
NT	017	ALV-3891-1459-003-006	GREGG	1176
NT	018	RBDASS05-H05-0818-1450-101-004-1316	VERILL	1316
NT	019	RBDASS05-H16-0901-2356-202-021-1918	BALANUS	1918
NT	020	ALV-4162-1457-001-003-2086	PICKETT	2086
NT	030	ALV-3890-1407-003-001	MANNING	1778
NT	031	ALV-3891-1459-003-009	GREGG	1176
NT	032	ALV-3890-1742-007-001	MANNING	1381

Table 4.2 Clumped Isotope Measurements

	SAMPLE	COUNT	AVERAGE	STDEV	STDERR	DEPTH (m)
YOUNGER DRYAS	NT 002	5	-1.5	2.9	1.3	2529
YOUNGER DRYAS	NT 010	8	-1.1	1.7	0.6	2372
YOUNGER DRYAS	NT 017	5	0.3	3.6	1.6	1176
YOUNGER DRYAS	NT 020	8	0.5	4.9	1.7	2086
YOUNGER DRYAS	NT 030	20	0.5	4.6	1.0	1778
HEINRICH 1	NT 031	6	1.7	3.3	1.4	1176
HEINRICH 1	NT 032	7	-0.2	3.0	1.1	1381
HEINRICH 1	NT 012	5	-0.7	5.0	2.3	1713
HEINRICH 1	NT 007	7	-1.2	3.4	1.3	2027
HEINRICH 1	NT 013	14	1.6	-4.1	-1.1	2265
HEINRICH 1	NT 016	15	3.5	2.6	0.7	2593
EARLY H1	NT 014	9	1.3	4.8	1.6	1886
EARLY H1	NT 015	9	-0.8	3.4	1.1	2459
EARLY H1	NT 006	3	-1.1	1.6	0.9	1427
BOLLING/ALLEROD	NT 018	4	3.1	1.2	0.6	1316

Table 4.3														
name	date	d47	d47err	FullD47	D47err	d48	FullD48	d13C	d18O	D47	Stretched D47	Acid corrected D47	Standard Corrected D47	T
NT012	April-10	13.6150	0.0171	0.1721	0.0095	58.4758	25.4124	-6.5293	41.3673	0.6127	0.7029	0.7829	0.7818	-1.4
NT012	April-10	13.8559	0.0162	0.1506	0.0104	58.2766	25.0367	-6.3553	41.4599	0.5859	0.6722	0.7522	0.7501	4.1
NT012	April-10	13.7490	0.0192	0.1465	0.0094	58.3591	25.1672	-6.4340	41.4343	0.5842	0.6702	0.7502	0.7480	4.5
NT013	April-10	13.1041	0.0113	0.1449	0.0088	58.8208	25.3744	-7.2139	41.5580	0.5966	0.6844	0.7644	0.7627	1.9
NT013	April-10	13.0673	0.0156	0.1515	0.0094	58.7911	25.3781	-7.2414	41.5416	0.6040	0.6929	0.7729	0.7715	0.3
NT013	April-10	13.1023	0.0190	0.1262	0.0100	58.5929	25.2176	-7.1635	41.5255	0.5779	0.6630	0.7430	0.7406	5.8
NT 014	April-10	14.1518	0.0136	0.1733	0.0099	60.8201	26.4465	-6.6184	41.9956	0.6023	0.6909	0.7709	0.7695	0.7
NT 014	April-10	14.1192	0.0116	0.1613	0.0076	60.4212	26.0814	-6.6285	41.9850	0.5909	0.6779	0.7579	0.7560	3.1
NT 014	April-10	13.7587	0.0423	0.1391	0.0109	59.3339	25.4192	-6.7061	41.8219	0.5766	0.6614	0.7414	0.7390	6.1
NT 015	April-10	18.8515	0.0126	0.2574	0.0079	65.0206	28.0563	-3.1758	43.2323	0.5840	0.6699	0.7499	0.7478	4.5
NT 015	April-10	18.9207	0.0147	0.2600	0.0085	64.9233	27.9251	-3.1271	43.2509	0.5852	0.6713	0.7513	0.7492	4.3
NT 016	April-10	17.3602	0.0134	0.2355	0.0106	63.9554	27.6709	-4.3414	42.9083	0.5946	0.6821	0.7621	0.7604	2.3
NT 016	April-10	17.0993	0.0108	0.2269	0.0101	63.6578	27.4826	-4.5470	42.8583	0.5917	0.6788	0.7588	0.7569	2.9
NT 016	April-10	17.7141	0.0124	0.2473	0.0099	64.0952	27.5258	-4.1371	43.0500	0.5987	0.6868	0.7668	0.7652	1.4
NT 017	April-10	16.8563	0.0111	0.2319	0.0084	59.0975	25.5606	-3.5179	41.5911	0.6019	0.6905	0.7705	0.7691	0.8
NT 018	April-10	15.6313	0.0142	0.1864	0.0087	58.8818	25.5159	-4.6358	41.5104	0.5832	0.6690	0.7490	0.7468	4.7
NT 018	April-10	15.3945	0.0123	0.1922	0.0096	58.2708	25.1616	-4.7610	41.3898	0.5941	0.6815	0.7615	0.7597	2.4
NT 019	April-10	12.2227	0.0095	0.1209	0.0081	56.1129	24.1274	-7.3800	40.8581	0.5918	0.6789	0.7589	0.7571	2.9
NT 019	April-10	12.2340	0.0120	0.1628	0.0088	56.6165	24.6260	-7.4068	40.8530	0.6334	0.7266	0.8066	0.8064	-5.5
NT 020	April-10	18.9524	0.0138	0.2882	0.0089	62.9427	27.0406	-2.5943	42.7274	0.6127	0.7028	0.7828	0.7818	-1.4
NT 020	April-10	18.7998	0.0147	0.2654	0.0111	62.4374	26.6975	-2.6511	42.6536	0.5931	0.6804	0.7604	0.7586	2.6
NT 020	April-10	18.9561	0.0129	0.2709	0.0086	62.6102	26.7573	-2.5528	42.7080	0.5953	0.6829	0.7629	0.7612	2.1
102 GC AZ 01	April-10	3.1611	0.0100	-0.1458	0.0082	-2.4151	-1.1915	0.4909	24.3121	0.5222	0.5991	0.6791		
102 GC AZ 01	April-10	3.4705	0.0101	-0.1404	0.0096	-1.3628	-0.5868	0.5679	24.5421	0.5209	0.5976	0.6776		
102 GC AZ 01	April-10	3.4985	0.0095	-0.1243	0.0089	-1.2178	-0.5379	0.5289	24.5916	0.5364	0.6154	0.6954		
102 GC AZ 01	April-10	3.0765	0.0132	-0.1958	0.0094	-2.5988	-1.2154	0.5400	24.2298	0.4741	0.5439	0.6239		
102 GC AZ 01	April-10	2.9058	0.0171	-0.1682	0.0111	-3.1195	-1.4997	0.4604	24.1084	0.5054	0.5798	0.6598		
102 GC AZ 01	April-10	3.3326	0.0112	-0.1760	0.0093	-1.7927	-0.8917	0.5284	24.4781	0.4884	0.5602	0.6402		
102 GC AZ 01	April-10	3.1878	0.0120	-0.1654	0.0101	-2.1925	-0.9939	0.5256	24.3249	0.5021	0.5760	0.6560		
102 GC AZ 01	April-10	8.4493	0.0094	-0.0365	0.0090	23.5753	10.3795	-1.6886	31.6241	0.5165	0.5925	0.6725		
102 GC AZ 01	April-10	3.2916	0.0104	-0.1531	0.0092	-2.1030	-1.0272	0.5551	24.3880	0.5121	0.5875	0.6675		
45923	April-10	22.5068	0.0173	0.3114	0.0090	64.6841	27.8357	0.5453	43.1705	0.5585	0.6406	0.7206		
45923	April-10	22.2518	0.0117	0.3292	0.0090	64.5868	27.8556	0.3258	43.1135	0.5819	0.6675	0.7475		
CARRERA MARBLE	April-10	17.6862	0.0261	-0.1032	0.0097	42.4002	18.1079	2.2423	37.1054	0.2488	0.2854	0.3654		
CARRERA MARBLE	April-10	18.1655	0.0113	-0.0982	0.0087	44.1182	19.0909	2.3653	37.4591	0.2434	0.2792	0.3592		
NT 015	May-10	19.1828	0.0080	0.3366	0.0079	65.9220	28.7171	-3.0281	43.3380	0.6303	0.7111	0.7911	0.7980	-4.1
NT 016	May-10	16.7839	0.0082	0.2211	0.0080	63.9932	27.9376	-4.7951	42.7923	0.5717	0.6450	0.7250	0.7328	7.3
NT 016	May-10	17.5865	0.0087	0.2671	0.0094	64.4980	28.1372	-4.1733	42.9373	0.5986	0.6754	0.7554	0.7628	1.9
NT 016	May-10	17.3952	0.0098	0.2491	0.0090	63.3953	27.1520	-4.3084	42.8968	0.5852	0.6602	0.7402	0.7478	4.5
NT 019	May-10	12.4465	0.0082	0.1301	0.0076	56.8373	24.5836	-7.2879	40.9833	0.5838	0.6586	0.7386	0.7462	4.8

NT 019	May-10	12.2522	0.0090	0.1138	0.0090	56.3469	24.3219	-7.3594	40.8746	0.5721	0.6454	0.7254	0.7332	7.2
NT 019	May-10	12.2535	0.0076	0.1345	0.0069	56.8429	24.7064	-7.4291	40.9239	0.5927	0.6687	0.7487	0.7562	3.0
NT 020	May-10	17.5151	0.0089	0.2567	0.0087	60.5126	25.8979	-3.4040	42.1159	0.5899	0.6656	0.7456	0.7531	3.6
NT 020	May-10	17.9501	0.0089	0.2518	0.0082	60.9526	25.9729	-3.1365	42.2934	0.5747	0.6484	0.7284	0.7361	6.7
NT 020	May-10	17.6691	0.0088	0.2669	0.0086	60.8387	25.9315	-3.4031	42.2589	0.5965	0.6729	0.7529	0.7604	2.3
45923	May-10	22.7568	0.0087	0.3822	0.0083	66.1025	29.0188	0.6299	43.2651	0.5910	0.6668	0.7468		
45923	May-10	22.6945	0.0084	0.3677	0.0082	65.7893	28.7448	0.5966	43.2509	0.5779	0.6520	0.7320		
CARRERA MARBLE	May-10	18.1654	0.0089	-0.0966	0.0092	44.3796	19.2216	2.2986	37.5226	0.2212	0.2496	0.3296		
CARRERA MARBLE	May-10	18.1619	0.0096	-0.0748	0.0092	43.6746	18.7395	2.3799	37.4175	0.2431	0.2742	0.3542		
CARRERA MARBLE	May-10	18.2243	0.0089	-0.1013	0.0085	43.4714	18.4027	2.3991	37.4879	0.2151	0.2427	0.3227		
CARRERA MARBLE	May-10	18.2222	0.0084	-0.0779	0.0078	45.2029	20.1007	2.3766	37.4839	0.2385	0.2691	0.3491		
NT 017	July-10	16.5115	0.0101	0.2334	0.0097	57.5415	24.4994	-3.6410	41.3646	0.6003	0.6761	0.7561	0.7895	-2.7
NT 017	July-10	16.5204	0.0092	0.2118	0.0090	57.3946	24.3010	-3.6385	41.3931	0.5785	0.6515	0.7315	0.7618	2.0
NT 017	July-10	16.6438	0.0104	0.2419	0.0103	57.5671	24.4715	-3.5419	41.3915	0.6057	0.6822	0.7622	0.7963	-3.9
NT 006	July-10	12.5838	0.0111	0.1347	0.0099	56.0217	23.7546	-7.1721	41.0025	0.5928	0.6676	0.7476	0.7800	-1.1
NT 006	July-10	12.5775	0.0125	0.1421	0.0109	55.8679	23.6096	-7.1843	41.0004	0.6004	0.6762	0.7562	0.7896	-2.7
NT 006	July-10	12.6660	0.0147	0.1292	0.0103	55.9294	23.5051	-7.1650	41.0838	0.5855	0.6594	0.7394	0.7707	0.5
NT 007	July -10	12.6873	0.0197	0.1287	0.0108	56.6072	23.4735	-7.4975	41.4351	0.5845	0.6583	0.7383	0.7694	0.7
NT 007	July-10	12.7319	0.0154	0.1555	0.0097	57.2628	24.1144	-7.4765	41.4320	0.6102	0.6872	0.7672	0.8020	-4.8
NT 007	July-10	12.6487	0.0113	0.1530	0.0076	57.0266	23.9313	-7.5353	41.4089	0.6097	0.6866	0.7666	0.8013	-4.7
NT 023	July-10	11.1165	0.0116	0.1045	0.0090	53.7416	22.8493	-7.9663	40.3391	0.5967	0.6720	0.7520	0.7849	-2.0
NT 023	July-10	11.0353	0.0095	0.1042	0.0092	53.0380	22.2656	-7.9978	40.2888	0.5983	0.6738	0.7538	0.7869	-2.3
NT 023	July-10	11.0607	0.0107	0.1014	0.0105	53.7114	22.8587	-8.0003	40.3194	0.5950	0.6701	0.7501	0.7827	-1.6
102 GC AZ 01	July-10	2.9856	0.0174	-0.2034	0.0106	-2.7939	-1.2452	0.5543	24.1695	0.4778	0.5381	0.6181		
45923	July-10	21.5692	0.0165	0.3171	0.0110	62.6157	26.6294	-0.0066	42.7699	0.5665	0.6380	0.7180		
45923	July-10	22.1773	0.0338	0.3209	0.0089	63.1122	26.8165	0.4574	42.9174	0.5561	0.6263	0.7063		
CARMEL CHALK	July-10	11.4389	0.0085	0.0153	0.0083	35.5768	15.6774	-2.0731	34.9490	0.5000	0.5631	0.6431		
CARMEL CHALK	July-10	11.4507	0.0113	0.0179	0.0106	34.7876	14.8993	-2.0659	34.9510	0.5024	0.5658	0.6458		
CARMEL CHALK	July-10	11.3842	0.0184	-0.0011	0.0091	34.6696	14.8396	-2.0863	34.9210	0.4850	0.5462	0.6262		
CARRERA MARBLE	July-10	18.0164	0.0171	-0.0880	0.0108	43.2449	18.5665	2.3734	37.2916	0.2439	0.2747	0.3547		
CARRERA MARBLE	July-10	18.0475	0.0105	-0.0694	0.0104	43.0958	18.3862	2.3676	37.3095	0.2618	0.2948	0.3748		
NT 012	September-10	9.3527	0.0095	-0.0240	0.0093	48.0929	18.6703	-8.9515	39.6846	0.5391	0.6032	0.6832	0.7029	13.0
NT 013	September-10	12.9000	0.0101	0.1251	0.0101	53.7629	20.8358	-7.2060	41.3846	0.6151	0.6883	0.7683	0.7932	-3.3
NT 016	September-10	16.3196	0.0088	0.1530	0.0085	57.5599	22.3417	-4.8675	42.4864	0.5727	0.6408	0.7208	0.7428	5.4
NT 016	September-10	16.8338	0.0106	0.1754	0.0101	57.8357	22.3877	-4.4808	42.5981	0.5845	0.6540	0.7340	0.7569	2.9
NT 016	September-10	16.7086	0.0105	0.1965	0.0101	58.8302	23.3819	-4.6131	42.5816	0.6081	0.6804	0.7604	0.7849	-2.0
NT 016	September-10	16.5168	0.0106	0.1826	0.0108	58.1105	22.7991	-4.7359	42.5243	0.5983	0.6694	0.7494	0.7732	0.0
NT 016	September-10	16.4594	0.0103	0.1559	0.0099	58.0752	22.7640	-4.7673	42.5249	0.5727	0.6408	0.7208	0.7429	5.4
NT 016	September-10	16.1942	0.0101	0.1522	0.0099	58.0472	22.8754	-4.9621	42.4545	0.5744	0.6427	0.7227	0.7449	5.1
NT 016	September-10	15.6688	0.0087	0.1358	0.0082	57.5797	22.7069	-5.3344	42.3109	0.5688	0.6365	0.7165	0.7383	6.3
NT 016	September-10	17.0630	0.0105	0.1624	0.0106	59.4628	23.7390	-4.3479	42.7105	0.5668	0.6342	0.7142	0.7359	6.7
NT 016	September-10	16.5688	0.0093	0.1696	0.0084	58.3871	23.0522	-4.6768	42.5316	0.5841	0.6536	0.7336	0.7564	3.0

NT 017	September-10	16.5371	0.0100	0.1590	0.0094	53.8769	20.8837	-3.5615	41.4083	0.5742	0.6425	0.7225	0.7446	5.1
NT 019	September-10	11.7572	0.0095	0.0671	0.0092	51.1525	19.9278	-7.4743	40.5566	0.5807	0.6497	0.7297	0.7523	3.7
NT 019	September-10	12.0048	0.0085	0.1146	0.0084	51.2559	19.8261	-7.3748	40.6596	0.6230	0.6971	0.7771	0.8026	-4.9
NT 019	September-10	11.8383	0.0100	0.0983	0.0099	51.4172	20.1968	-7.4174	40.5503	0.6102	0.6827	0.7627	0.7873	-2.4
NT 019	September-10	11.8697	0.0098	0.0897	0.0091	51.4138	20.1163	-7.4164	40.5899	0.6010	0.6724	0.7524	0.7764	-0.5
NT 019	September-10	11.8608	0.0081	0.0735	0.0079	51.5017	20.1762	-7.4216	40.6026	0.5850	0.6545	0.7345	0.7574	2.8
NT 019	September-10	11.5814	0.0082	0.0559	0.0083	51.5381	20.4281	-7.5770	40.4924	0.5731	0.6412	0.7212	0.7433	5.3
NT 019	September-10	11.4845	0.0092	0.0781	0.0091	51.5381	20.4136	-7.7064	40.5001	0.5973	0.6683	0.7483	0.7720	0.2
NT 019	September-10	11.5184	0.0087	0.0892	0.0086	51.4734	20.3655	-7.6756	40.4926	0.6077	0.6800	0.7600	0.7844	-1.9
NT 007	September-10	12.7405	0.0093	0.0940	0.0091	54.7174	21.6012	-7.4189	41.4665	0.5873	0.6571	0.7371	0.7602	2.3
NT 007	September-10	12.6027	0.0090	0.1240	0.0088	54.3527	21.3566	-7.5344	41.4111	0.6202	0.6939	0.7739	0.7992	-4.3
NT 007	September-10	12.5979	0.0114	0.0880	0.0114	54.3897	21.4086	-7.4936	41.4029	0.5843	0.6537	0.7337	0.7566	3.0
NT 024	September-10	13.2076	0.0091	0.1060	0.0084	53.0818	20.9372	-6.4789	40.9943	0.5897	0.6598	0.7398	0.7630	1.8
NT 024	September-10	13.2983	0.0084	0.1105	0.0083	53.0134	20.7859	-6.4348	41.0375	0.5923	0.6627	0.7427	0.7661	1.3
NT 024	September-10	13.4221	0.0101	0.1360	0.0103	53.4110	21.0800	-6.3819	41.0840	0.6153	0.6884	0.7684	0.7934	-3.4
102 GC AZ 01	September-10	2.9597	0.0080	-0.1998	0.0079	-2.5428	-0.9225	0.5590	24.1183	0.4948	0.5536	0.6336		
45923	September-10	22.0784	0.0096	0.2784	0.0097	58.6715	22.5411	0.4183	42.9208	0.5796	0.6485	0.7285		
45923	September-10	22.0303	0.0090	0.2986	0.0086	58.8857	22.6715	0.3084	42.9601	0.6008	0.6722	0.7522		
45923	September-10	22.3554	0.0099	0.2687	0.0093	59.8257	23.4460	0.6014	43.0276	0.5641	0.6312	0.7112		
CARMEL CHALK	September-10	11.3024	0.0084	-0.0355	0.0082	32.7104	12.8832	-2.1416	34.9504	0.4875	0.5454	0.6254		
CARMEL CHALK	September-10	11.2734	0.0081	-0.0338	0.0077	32.2987	12.6008	-2.1094	34.8884	0.4897	0.5479	0.6279		
CARMEL CHALK	September-10	11.3266	0.0097	-0.0496	0.0092	32.8911	13.0338	-2.1160	34.9641	0.4729	0.5291	0.6091		
CARRERA MARBLE	September-10	17.9175	0.0098	-0.1402	0.0099	40.5811	16.0458	2.3785	37.2611	0.2466	0.2759	0.3559		
CARRERA MARBLE	September-10	17.8768	0.0102	-0.1418	0.0098	40.5237	16.0706	2.3808	37.2196	0.2459	0.2751	0.3551		
NT 014	December-10	13.5725	0.0107	0.1435	0.0103	52.4127	18.9666	-6.8294	41.6709	0.6214	0.6991	0.7791	0.7991	-4.3
NT 014	December-10	9.6418	0.0113	-0.0043	0.0094	46.9956	17.3485	-8.8084	39.8149	0.5527	0.6218	0.7018	0.7235	9.0
NT 015	December-10	18.6215	0.0086	0.2264	0.0082	56.2795	19.8904	-3.2269	43.1034	0.6025	0.6779	0.7579	0.7784	-0.8
NT 030	December-10	13.1703	0.0104	0.1226	0.0105	48.7597	17.0199	-6.3924	40.8544	0.6085	0.6847	0.7647	0.7850	-2.0
NT 030	December-10	12.4964	0.0094	0.0521	0.0095	47.7294	16.4005	-6.8106	40.6606	0.5516	0.6207	0.7007	0.7223	9.2
NT 030	December-10	12.6926	0.0087	0.1206	0.0082	48.7852	17.3026	-6.7443	40.7229	0.6161	0.6932	0.7732	0.7934	-3.4
NT 030	December-10	12.6633	0.0097	0.0907	0.0096	48.4107	16.9741	-6.7253	40.7053	0.5868	0.6603	0.7403	0.7611	2.1
NT 030	December-10	12.7142	0.0087	0.1338	0.0084	48.5109	16.9585	-6.7764	40.7631	0.6289	0.7077	0.7877	0.8075	-5.7
NT 031	December-10	13.4632	0.0082	0.1010	0.0081	48.2329	16.7295	-5.9565	40.7404	0.5810	0.6537	0.7337	0.7547	3.3
NT 031	December-10	13.4501	0.0093	0.0965	0.0092	48.7340	17.1596	-5.9941	40.7690	0.5768	0.6490	0.7290	0.7501	4.1
NT 031	December-10	13.3871	0.0106	0.1025	0.0102	48.8622	17.4358	-5.9859	40.6913	0.5841	0.6572	0.7372	0.7581	2.7
NT 031	December-10	13.3699	0.0095	0.1352	0.0093	48.8641	17.4273	-6.1279	40.6998	0.6171	0.6943	0.7743	0.7944	-3.5
NT 031	December-10	13.3294	0.0081	0.0905	0.0079	48.3313	16.9300	-6.0278	40.6868	0.5732	0.6450	0.7250	0.7461	4.8
NT 031	December-10	13.6864	0.0096	0.1288	0.0094	48.8218	17.1505	-5.8353	40.8169	0.6043	0.6799	0.7599	0.7803	-1.2
NT 032	December-10	17.5139	0.0095	0.1690	0.0094	53.3984	18.3424	-3.6541	42.4715	0.5674	0.6384	0.7184	0.7397	6.0
NT 032	December-10	17.4767	0.0094	0.1405	0.0095	53.6064	18.5504	-3.6593	42.4681	0.5397	0.6072	0.6872	0.7092	11.8
NT 032	December-10	17.6603	0.0092	0.2129	0.0091	54.5984	19.3342	-3.6378	42.5575	0.6083	0.6845	0.7645	0.7848	-1.9
NT 032	December-10	17.6070	0.0097	0.2197	0.0095	54.5393	19.3776	-3.6473	42.5060	0.6162	0.6934	0.7734	0.7935	-3.4
NT 012	December-10	9.7513	0.0090	-0.0214	0.0086	46.0164	16.3437	-8.7065	39.8421	0.5334	0.6002	0.6802	0.7023	13.1
NT 012	December-10	9.5236	0.0088	-0.0037	0.0088	46.0222	16.5435	-8.8569	39.7431	0.5557	0.6252	0.7052	0.7268	8.4

NT 014	December-10	13.3426	0.0092	0.1512	0.0089	51.6131	18.4146	-6.9568	41.5573	0.6336	0.7129	0.7929	0.8127	-6.5
NT 015	December-10	18.5675	0.0091	0.2244	0.0088	56.2006	19.8304	-3.2715	43.0951	0.6016	0.6769	0.7569	0.7774	-0.7
45923	December-10	22.3602	0.0091	0.2442	0.0088	55.5144	19.1528	0.5641	43.0941	0.5450	0.6132	0.6932		
45923	December-10	22.5466	0.0102	0.2989	0.0100	56.6689	20.1291	0.6251	43.1650	0.5959	0.6705	0.7505		
45923	December-10	22.3900	0.0095	0.2810	0.0090	56.1402	19.6824	0.5175	43.1326	0.5811	0.6539	0.7339		
CARRERA MARBLE	December-10	18.0107	0.0097	-0.1827	0.0094	38.0786	13.3443	2.3828	37.3933	0.2057	0.2315	0.3115		
CARRERA MARBLE	December-10	17.9624	0.0090	-0.2090	0.0087	37.7671	13.1202	2.4028	37.3521	0.1804	0.2030	0.2830		
CARRERA MARBLE	December-10	18.0128	0.0093	-0.1705	0.0094	38.3951	13.6735	2.3828	37.3830	0.2178	0.2451	0.3251		
CARRERA MARBLE	December-10	18.0048	0.0086	-0.1654	0.0080	38.3530	13.6999	2.4046	37.3481	0.2231	0.2510	0.3310		
CARRERA MARBLE	December-10	17.9825	0.0104	-0.1395	0.0099	38.3986	13.8339	2.4019	37.3024	0.2495	0.2807	0.3607		
NT 012	February-11	10.0859	0.0109	-0.0885	0.0100	40.2082	10.3465	-8.5193	40.0543	0.5804	0.6328	0.7128	0.7234	9.0
NT 012	February-11	9.6742	0.0087	-0.1133	0.0085	39.8487	10.2374	-8.7895	39.9311	0.5599	0.6105	0.6905	0.6999	13.6
NT 012	February-11	9.7463	0.0106	-0.0930	0.0101	40.2167	10.5507	-8.7598	39.9538	0.5794	0.6318	0.7118	0.7223	9.3
NT 012	February-11	9.6031	0.0108	-0.0920	0.0100	40.0035	10.5141	-8.8183	39.8661	0.5819	0.6346	0.7146	0.7252	8.7
NT 032	February-11	16.7781	0.3246	0.0301	0.0132	46.5807	12.0532	-3.5986	42.6299	0.6283	0.6852	0.7652	0.7784	-0.8
NT 032	February-11	17.4946	0.0090	0.0390	0.0085	47.1295	12.1232	-3.6621	42.5839	0.6297	0.6867	0.7667	0.7800	-1.1
NT 032	February-11	17.5677	0.0097	0.0365	0.0095	46.7588	11.6366	-3.6524	42.6500	0.6265	0.6831	0.7631	0.7762	-0.5
NT 032	February-11	17.4828	0.0099	0.0319	0.0094	47.2823	12.2283	-3.6894	42.6060	0.6227	0.6790	0.7590	0.7719	0.3
45923	February-11	22.2565	0.0087	0.0692	0.0087	48.0056	11.7301	0.5103	43.2135	0.6097	0.6648	0.7448		
CARRERA MARBLE	February-11	18.0290	0.0127	-0.3227	0.0112	33.4163	8.5016	2.3535	37.5735	0.2624	0.2861	0.3661		
CARRERA MARBLE	February-11	18.0184	0.0112	-0.3328	0.0098	33.8686	8.9271	2.3449	37.5819	0.2524	0.2753	0.3553		
CARRERA MARBLE	February-11	18.0379	0.0113	-0.1088	0.0109	39.7288	15.0239	2.3695	37.3581	0.4762	0.5193	0.5993		
TV01	February-11	11.3254	0.0084	-0.0897	0.0079	14.6117	3.7987	2.5028	30.4878	0.5661	0.6173	0.6973		
TV01	February-11	11.3236	0.0113	-0.1288	0.0101	15.0068	4.0605	2.4735	30.5541	0.5270	0.5746	0.6546		
NT 012	April-11	9.9732	0.0099	0.0327	0.0099	65.2537	34.9888	-8.5591	39.8650	0.5991	0.5980	0.6780	0.7124	11.2
NT 014	April-11	13.1407	0.0108	0.1785	0.0110	72.7511	39.1539	-7.0545	41.4228	0.6558	0.6545	0.7345	0.7744	-0.2
NT 014	April-11	13.6076	0.0119	0.1924	0.0114	73.1311	39.0107	-6.8519	41.6788	0.6567	0.6554	0.7354	0.7753	-0.3
NT 014	April-11	13.3026	0.0135	0.1476	0.0126	73.4421	39.6319	-6.9545	41.5185	0.6204	0.6191	0.6991	0.7356	6.8
NT 014	April-11	13.2890	0.0115	0.1471	0.0111	71.8669	38.2070	-6.9166	41.4680	0.6203	0.6190	0.6990	0.7355	6.8
NT 014	April-11	17.8542	0.0147	-0.0973	0.0136	52.2669	27.5454	2.3150	37.2160	0.2475	0.2470	0.3270	0.3279	139.3
NT 015	April-11	18.9526	0.0096	0.3400	0.0094	81.0040	43.6584	-3.0606	43.1553	0.6538	0.6525	0.7325	0.7722	0.2
NT 015	April-11	18.4143	0.0127	0.3498	0.0122	80.1896	43.3589	-3.3719	42.9123	0.6788	0.6775	0.7575	0.7995	-4.4
NT 015	April-11	18.8593	0.0102	0.3486	0.0097	79.1007	42.0529	-3.0464	43.0390	0.6651	0.6638	0.7438	0.7845	-1.9
NT 015	April-11	18.5192	0.0127	0.3543	0.0118	79.6495	42.7158	-3.3314	42.9730	0.6804	0.6790	0.7590	0.8012	-4.7
NT 018	April-11	15.1693	0.0094	0.2238	0.0088	73.0780	39.8722	-4.8271	41.2164	0.6441	0.6428	0.7228	0.7615	2.1
NT 018	April-11	15.3413	0.0129	0.2216	0.0123	72.9436	39.7072	-4.6670	41.2335	0.6371	0.6358	0.7158	0.7539	3.4
NT 018	April-11	12.5918	0.0120	0.1300	0.0112	66.2062	34.3845	-6.7630	40.6304	0.6228	0.6215	0.7015	0.7382	6.3
NT 030	April-11	12.6858	0.0101	0.1843	0.0096	70.1282	38.1366	-6.7503	40.6568	0.6744	0.6731	0.7531	0.7947	-3.6
NT 030	April-11	12.6011	0.0104	0.1822	0.0102	70.6186	38.6850	-6.7975	40.6206	0.6748	0.6734	0.7534	0.7951	-3.7
NT 030	April-11	12.6704	0.0123	0.1706	0.0117	68.3107	36.5891	-6.6419	40.5481	0.6612	0.6599	0.7399	0.7802	-1.2
45923	April-11	22.3721	0.0144	0.4097	0.0136	77.7985	40.8873	0.5154	42.9846	0.6274	0.6262	0.7062		
45924	April-11	22.2118	0.0092	0.4181	0.0088	80.0823	43.0951	0.3446	42.9841	0.6403	0.6391	0.7191		

45925	April-11	22.9073	0.0087	0.4208	0.0081	81.0087	43.5318	0.8169	43.2119	0.6235	0.6223	0.7023		
CARMEL CHALK	April-11	11.4073	0.0132	-0.0045	0.0126	42.8289	22.8077	-2.0659	34.9504	0.5216	0.5206	0.6006		
CARRERA MARBLE	April-11	17.9981	0.0094	-0.0473	0.0092	53.6301	28.7796	2.3601	37.2648	0.2934	0.2928	0.3728		
CARRERA MARBLE	April-11	18.0488	0.0101	-0.0770	0.0100	53.8107	28.8174	2.3715	37.3348	0.2623	0.2618	0.3418		
CARRERA MARBLE	April-11	18.0342	0.0109	-0.0926	0.0106	52.4764	27.5170	2.3741	37.3335	0.2472	0.2467	0.3267		
CARRERA MARBLE	April-11	17.5697	0.0089	-0.0771	0.0085	51.8898	27.5889	2.2156	37.0081	0.2757	0.2751	0.3551		
TV01	April-11	11.3187	0.0116	0.0299	0.0113	22.6202	11.8971	2.5036	30.3684	0.5585	0.5574	0.6374		
TV01	April-11	11.1381	0.0119	0.0294	0.0113	22.6379	12.1287	2.4303	30.2595	0.5631	0.5620	0.6420		
NT 012	September-11	12.6621	0.0084	0.1373	0.0082	56.6058	24.2974	-7.1238	41.0839	0.7104	0.7137	0.7937	0.8172	-7.2
NT 012	September-11	11.9269	0.0074	0.1021	0.0072	55.4389	23.4195	-7.7073	40.9564	0.6907	0.6939	0.7739	0.7951	-3.7
NT 013	September-11	18.8498	0.0101	0.2719	0.0096	63.8077	27.1232	-3.0868	43.1806	0.7139	0.7171	0.7971	0.8211	-7.9
NT 013	September-11	13.7802	0.0088	0.1326	0.0087	58.7062	25.2659	-6.5268	41.6248	0.6820	0.6851	0.7651	0.7853	-2.0
NT 013	September-11	12.9658	0.0104	0.1063	0.0099	55.2360	22.7550	-6.8923	41.1926	0.6729	0.6760	0.7560	0.7751	-0.3
NT 013	September-11	12.5919	0.0084	0.0878	0.0079	56.5262	24.0878	-7.2121	41.1515	0.6623	0.6654	0.7454	0.7632	1.8
NT 013	September-11	12.2790	0.0100	0.0768	0.0096	55.3178	23.3484	-7.2979	40.9318	0.6580	0.6610	0.7410	0.7583	2.6
NT 013	September-11	12.2603	0.0127	0.0732	0.0120	54.9967	23.0351	-7.3144	40.9325	0.6548	0.6578	0.7378	0.7547	3.3
NT 013	September-11	16.4930	0.0093	0.1660	0.0089	60.4187	25.1302	-4.7181	42.5329	0.6579	0.6609	0.7409	0.7582	2.7
NT 013	September-11	12.5995	0.0120	0.0771	0.0113	55.9964	23.6570	-7.1510	41.1091	0.6515	0.6545	0.7345	0.7510	4.0
NT 013	September-11	16.9540	0.0092	0.1664	0.0090	61.3194	25.6725	-4.4179	42.6993	0.6485	0.6515	0.7315	0.7476	4.6
NT 013	September-11	16.6990	0.0083	0.1398	0.0079	61.2595	25.8285	-4.5399	42.5905	0.6273	0.6301	0.7101	0.7237	9.0
NT 020	September-11	14.5559	0.4273	0.1490	0.0140	58.1793	25.0378	-5.6073	41.4780	0.6819	0.6851	0.7651	0.7852	-2.0
NT 020	September-11	17.4042	0.2822	0.2518	0.0104	60.2664	25.6305	-3.5439	42.2001	0.7244	0.7277	0.8077	0.8329	-9.7
NT 007	September-11	12.6860	0.0096	0.1035	0.0090	57.3689	24.1364	-7.5280	41.5429	0.6761	0.6792	0.7592	0.7787	-0.9
45923	September-11	22.8291	0.0111	0.2913	0.0105	63.1518	26.2163	0.8051	43.3110	0.6489	0.6519	0.7317		
45924	September-11	22.9039	0.0112	0.3193	0.0106	65.5247	28.4314	0.8135	43.3491	0.6753	0.6784	0.7583		
45925	September-11	23.9871	0.0097	0.2010	0.0092	64.8294	27.9882	0.5865	43.2340	0.5340	0.5365	0.6165		
CARRERA MARBLE	September-11	17.9510	0.0101	-0.1932	0.0097	43.6186	18.8680	2.3659	37.3938	0.2678	0.2690	0.3489		
CARRERA MARBLE	September-11	17.8912	0.0104	-0.2003	0.0097	43.0360	18.3859	2.3573	37.3495	0.2619	0.2631	0.3431		
CARRERA MARBLE	September-11	18.6397	0.2192	-0.0936	0.0241	46.2773	19.9230	2.1738	38.1698	0.3528	0.3544	0.4343		
CARRERA MARBLE	September-11	17.9951	0.0088	-0.1791	0.0087	43.3756	18.5783	2.3691	37.4206	0.2809	0.2822	0.3621		
TV01	September-11	11.5029	0.0098	0.0260	0.0094	20.0074	9.1565	2.5881	30.5073	0.6236	0.6265	0.7064		
TV01	September-11	11.4582	0.0096	0.0320	0.0093	19.8296	8.9847	2.5379	30.5053	0.6306	0.6335	0.7134		
NT 023	October-11	10.8268	0.0099	-0.1661	0.0107	33.8010	3.3037	-8.1025	40.5090	0.7029	0.6740	0.7540	0.7861	-2.2
NT 023	October-11	13.0399	0.0098	-0.1680	0.0097	35.4629	3.6096	-6.5260	41.1833	0.6984	0.6697	0.7497	0.7813	-1.3
NT 023	October-11	13.1265	0.0087	-0.1857	0.0096	35.7491	3.7584	-6.4871	41.2499	0.6806	0.6527	0.7327	0.7623	1.9
NT 023	October-11	10.8201	0.0074	-0.1837	0.0088	33.6907	3.2189	-8.0791	40.4973	0.6853	0.6571	0.7371	0.7673	1.1
NT 023	October-11	11.0534	0.0084	-0.1642	0.0096	33.6778	3.0666	-7.9345	40.5695	0.7045	0.6756	0.7556	0.7878	-2.4
NT 024	October-11	13.0565	0.0094	-0.1620	0.0105	35.6261	3.7446	-6.5275	41.1954	0.7044	0.6755	0.7555	0.7877	-2.4
NT 024	October-11	13.0827	0.0084	-0.1487	0.0082	36.3380	4.4489	-6.5069	41.1876	0.7176	0.6882	0.7682	0.8019	-4.8

45923	October-11	22.2340	0.0101	-0.2109	0.0095	40.0647	3.9718	0.7401	43.2919	0.6449	0.6184	0.6984		
45923	October-11	22.3402	0.0082	-0.1984	0.0085	40.0532	3.7186	0.7071	43.4176	0.6572	0.6302	0.7102		
CARRERA MARBLE	October-11	17.4551	0.0073	-0.5863	0.0081	25.7411	1.5143	2.3178	37.3431	0.2750	0.2637	0.3437		
CARRERA MARBLE	October-11	17.5486	0.0082	-0.6056	0.0085	26.2415	1.8531	2.3543	37.4209	0.2555	0.2451	0.3251		
CARRERA MARBLE	October-11	17.5788	0.0107	-0.5132	0.0098	27.3632	3.0469	2.3410	37.3698	0.3480	0.3337	0.4137		
CARRERA MARBLE	October-11	17.5096	0.0088	-0.5782	0.0107	27.5658	3.2432	2.3371	37.3706	0.2830	0.2714	0.3514		
CARRERA MARBLE	October-11	17.4110	0.0098	-0.5414	0.0171	28.7942	4.6604	2.3129	37.2583	0.3199	0.3068	0.3868		
TV01	October-11	11.0985	0.0086	-0.2520	0.0103	12.2499	1.4094	2.4200	30.5453	0.6167	0.5914	0.6714		
TV01	October-11	11.1803	0.0102	-0.2719	0.0104	11.8897	0.9815	2.4871	30.5820	0.5966	0.5721	0.6521		
NT 030	November-11	12.6919	0.0105	-0.0024	0.0103	39.5846	8.3509	-6.6521	40.7571	0.6362	0.6836	0.7636	0.7807	1.7
NT 030	November-11	11.7684	0.0083	0.0272	0.0082	39.7401	9.5029	-7.1028	40.2413	0.6765	0.7270	0.8070	0.8211	-5.6
NT 030	November-11	11.8886	0.0095	-0.0129	0.0090	39.5798	9.1675	-7.0321	40.3341	0.6350	0.6824	0.7624	0.7795	1.9
NT 030	November-11	11.8422	0.0106	-0.0316	0.0102	39.2909	8.9399	-7.0326	40.3066	0.6168	0.6629	0.7429	0.7614	5.4
NT 030	November-11	11.8313	0.0095	-0.0480	0.0094	39.6081	9.2043	-7.0496	40.3293	0.6006	0.6454	0.7254	0.7451	8.7
45923	November-11	22.3285	0.0097	0.0391	0.0092	45.3963	9.2367	0.6484	43.1899	0.5652	0.6074	0.6874		
CARRERA MARBLE	November-11	17.7672	0.0101	-0.3867	0.0095	30.8744	6.3802	2.3621	37.3781	0.1927	0.2071	0.2871		
CARRERA MARBLE	November-11	17.7456	0.0089	-0.3939	0.0084	30.7422	6.3116	2.3797	37.3469	0.1857	0.1995	0.2795		
CARRERA MARBLE	November-11	17.7518	0.0102	-0.3640	0.0100	31.0032	6.6086	2.3770	37.3253	0.2155	0.2316	0.3116		
CARRERA MARBLE	November-11	17.7518	0.0102	-0.3640	0.0100	31.0032	6.6086	2.3770	37.3253	0.2155	0.2316	0.3116		
CARRERA MARBLE	November-11	17.5860	0.0091	-0.3639	0.0081	30.8404	6.7184	2.3490	37.1865	0.2176	0.2338	0.3138		
TV01	November-11	11.1954	0.0090	-0.1491	0.0082	13.3828	2.7569	2.5431	30.3883	0.5069	0.5448	0.6248		
TV01	November-11	11.2988	0.0105	-0.1220	0.0105	13.6008	2.9446	2.6067	30.4024	0.5328	0.5726	0.6526		
TV01	November-11	11.0942	0.0086	-0.1608	0.0088	13.3247	2.9014	2.5581	30.2843	0.4964	0.5334	0.6134		
TV01	November-11	11.2704	0.0075	-0.0740	0.0070	14.3850	3.8301	2.5853	30.3464	0.5811	0.6245	0.7045		
NT 030	January-12	12.0863	0.0094	-0.0188	0.0082	42.5035	11.7772	-6.9431	40.4513	0.5564	0.6535	0.7335	0.7325	7.3
NT 030	January-12	12.1535	0.0099	0.0296	0.0093	42.7352	11.9813	-6.9354	40.4620	0.6040	0.7095	0.7895	0.7884	-2.5
NT 030	January-12	11.9847	0.0082	0.0073	0.0079	42.5622	11.8976	-7.0409	40.4190	0.5837	0.6857	0.7657	0.7646	1.5
NT 030	January-12	11.8485	0.0077	-0.0030	0.0069	42.4258	11.9107	-7.0936	40.3443	0.5751	0.6755	0.7555	0.7545	3.3
NT 030	January-12	11.9682	0.0095	0.0124	0.0084	42.8592	12.2821	-7.0128	40.3696	0.5890	0.6918	0.7718	0.7708	0.5
NT 030	January-12	12.0016	0.0119	0.0153	0.0101	42.7668	12.1249	-7.0171	40.4041	0.5916	0.6949	0.7749	0.7738	-0.1
NT 030	January-12	12.0675	0.0078	0.0387	0.0077	43.2609	12.5897	-6.9816	40.4116	0.6141	0.7214	0.8014	0.8003	-4.5
45923	January-12	22.9425	0.0095	0.1340	0.0089	50.7253	14.0975	1.0264	43.3351	0.5795	0.6807	0.7607		
CARMEL CHALK	January-12	11.3532	0.0096	-0.1189	0.0092	27.5098	7.6940	-2.0694	35.0159	0.4651	0.5464	0.6264		
CARRERA MARBLE	January-12	17.8568	0.0084	-0.2704	0.0082	34.5584	10.0435	2.3678	37.3439	0.2359	0.2771	0.3571		
TV01	January-12	11.3832	0.0098	-0.0782	0.0086	15.1171	4.3202	2.5820	30.4666	0.5054	0.5937	0.6737		
TV01	January-12	11.2733	0.0107	-0.0967	0.0088	15.0897	4.3511	2.5186	30.4369	0.4882	0.5735	0.6535		

Table 4.4 Heated Gases

Date	d47	d47 stdev	D47	D47 stderr	d48	D48	D48 stdev
April-10	28.567	0.060	-0.116	0.012	128.971	53.513	0.880
April-10	-4.799	0.103	-0.851	0.007	10.199	4.099	0.300
April-10	-3.958	0.075	-0.817	0.012	12.273	5.179	0.205
April-10	27.925	0.014	-0.132	0.011	125.961	52.129	0.633
April-10	-2.320	0.015	-0.786	0.011	18.606	7.996	0.272
April-10	25.145	0.035	-0.180	0.013	116.299	48.616	0.684
April-10	-4.942	0.035	-0.826	0.008	8.749	3.648	0.123
April-10	-3.127	0.032	-0.822	0.015	15.518	6.541	0.174
April-10	26.648	0.020	-0.163	0.008	120.466	49.515	0.388
May-10	24.335	0.064	-0.146	0.011	114.441	48.778	1.788
May-10	-3.406	0.076	-0.807	0.010	15.045	6.604	0.348
May-10	23.563	0.074	-0.199	0.010	110.968	46.609	1.288
May-10	-3.449	0.060	-0.852	0.009	14.713	6.325	0.306
May-10	22.432	0.059	-0.234	0.007	107.796	46.056	1.147
July-10	27.648	0.021	-0.088	0.008	124.692	51.808	1.170
July-10	-3.422	0.016	-0.812	0.013	15.457	6.714	0.283
July-10	26.276	0.029	-0.125	0.013	120.198	50.105	0.784
July-10	26.985	0.017	-0.163	0.012	119.701	48.283	0.829
July-10	-3.214	0.017	-0.844	0.010	15.559	6.661	0.434
July-10	9.669	0.016	-0.526	0.013	58.398	23.681	0.485
July-10	20.978	0.031	-0.257	0.012	100.124	41.812	0.656
September-10	25.103	0.016	-0.253	0.010	108.100	40.484	0.911
September-10	27.447	0.028	-0.232	0.010	115.565	43.145	0.976
September-10	26.634	0.016	-0.230	0.008	112.780	42.406	0.845
September-10	-2.279	0.013	-0.826	0.017	18.063	7.068	0.262
September-10	24.881	0.017	-0.239	0.011	106.959	40.621	0.607
September-10	25.589	0.015	-0.209	0.007	110.951	42.162	0.990
September-10	27.411	0.012	-0.199	0.015	116.367	44.196	0.915
September-10	-4.113	0.015	-0.808	0.012	11.797	4.757	0.157
September-10	25.289	0.011	-0.178	0.013	113.819	45.903	1.441
September-10	-3.359	0.022	-0.849	0.011	14.626	5.887	0.308
September-10	25.927	0.027	-0.218	0.019	112.601	43.413	0.593
September-10	-3.584	0.013	-0.820	0.015	13.758	5.658	0.288
September-10	25.952	0.021	-0.215	0.015	112.566	43.296	0.480
December-10	-3.092	0.017	-0.811	0.011	13.460	4.568	0.261
December-10	26.004	0.013	-0.236	0.013	104.155	34.756	0.327
December-10	-2.776	0.016	-0.823	0.020	14.379	4.859	0.364
December-10	16.299	0.016	-0.430	0.007	74.174	25.707	0.338
December-10	-3.621	0.032	-0.809	0.009	12.440	4.505	0.149
December-10	27.337	0.012	-0.203	0.015	108.433	36.778	0.263
December-10	27.086	0.009	-0.205	0.015	107.918	36.768	0.284
December-10	27.170	0.018	-0.193	0.004	109.105	37.500	0.260
December-10	27.233	0.014	-0.201	0.010	108.943	37.282	0.417
December-10	26.529	0.015	-0.213	0.009	107.290	36.959	0.131
February-11	-2.471	0.010	-0.792	0.009	13.670	3.592	0.567
February-11	24.096	0.022	-0.498	0.014	86.004	21.225	0.407
February-11	24.286	0.024	-0.505	0.012	85.813	20.701	0.492
February-11	-5.078	0.027	-0.833	0.010	7.210	2.027	0.263
February-11	-2.977	0.019	-0.784	0.013	12.135	3.031	0.282
February-11	25.440	0.019	-0.523	0.009	89.775	22.197	0.391
February-11	-3.972	0.023	-0.845	0.013	9.732	2.190	0.331
February-11	26.498	0.024	-0.516	0.014	92.313	22.410	0.377
April-11	-3.676	0.018	-0.955	0.014	16.676	8.185	0.903
April-11	27.087	0.017	-0.076	0.014	151.726	77.566	1.352
April-11	18.498	0.028	-0.318	0.016	114.863	60.253	1.767

April-11	19.757	0.033	-0.292	0.020	118.608	61.650	1.266
April-11	20.226	0.013	-0.283	0.016	123.199	65.321	1.711
April-11	-3.062	0.017	-0.938	0.012	18.875	9.894	1.187
April-11	-3.215	0.026	-0.924	0.015	18.823	9.504	1.042
April-11	17.870	0.020	-0.354	0.013	113.079	59.771	1.029
April-11	17.552	0.027	-0.359	0.019	109.589	57.139	1.781
September-11	17.458	0.023	-0.484	0.011	87.032	35.636	1.125
September-11	17.630	0.011	-0.491	0.010	88.168	36.380	0.825
September-11	15.501	0.020	-0.538	0.013	83.001	33.837	0.969
September-11	24.189	0.016	-0.289	0.014	110.991	45.515	1.020
September-11	-3.837	0.020	-0.973	0.009	14.410	6.543	1.412
September-11	23.195	0.012	-0.353	0.009	105.207	41.843	0.745
September-11	19.367	0.009	-0.466	0.013	91.771	37.119	0.939
September-11	20.623	0.022	-0.360	0.022	103.382	44.175	3.177
September-11	-4.886	0.027	-0.911	0.012	9.964	3.577	0.775
September-11	15.635	0.016	-0.490	0.017	81.408	33.030	0.931
September-11	-3.619	0.024	-0.933	0.007	16.035	7.104	1.084
September-11	-5.129	0.020	-0.942	0.013	9.207	3.557	0.661
September-11	23.159	0.022	-0.353	0.017	107.511	43.499	1.064
September-11	-6.663	0.015	-0.953	0.019	4.796	1.636	0.922
September-11	22.231	0.012	-0.380	0.011	104.243	42.334	0.736
October-11	21.707	0.015	-0.836	0.014	64.174	4.887	0.693
October-11	22.325	0.016	-0.873	0.016	65.802	5.069	0.547
October-11	21.520	0.040	-0.853	0.018	64.131	5.206	0.660
October-11	21.381	0.005	-0.863	0.018	63.860	5.176	0.766
October-11	-2.800	0.018	-0.889	0.012	10.812	0.722	0.578
October-11	-2.984	0.019	-0.887	0.017	10.373	0.601	0.619
October-11	-2.921	0.020	-0.879	0.015	11.162	1.327	0.526
November-11	18.125	7.324	-0.550	0.013	71.631	14.407	0.258
November-11	-3.458	0.029	-0.819	0.013	10.749	2.218	0.175
November-11	-2.847	0.044	-0.829	0.014	12.221	2.456	0.100
November-11	19.308	0.039	-0.550	0.014	68.169	14.040	0.323
November-11	20.802	0.034	-0.578	0.014	72.591	15.125	0.250
November-11	15.406	0.026	-0.622	0.010	58.119	12.216	0.126
November-11	20.695	0.013	-0.533	0.006	72.447	15.391	0.232
November-11	-3.400	0.029	-0.825	0.006	11.196	2.382	0.258
January-12	-5.997	0.020	-0.793	0.008	4.843	1.504	0.373
January-12	24.612	0.037	-0.402	0.014	89.322	23.851	0.270
January-12	27.002	9.547	-0.404	0.013	96.456	25.862	0.215
January-12	-3.869	0.026	-0.742	0.009	10.054	3.001	0.326
January-12	26.538	0.029	-0.417	0.010	94.898	24.860	0.157
January-12	-3.563	0.030	-0.785	0.011	10.756	2.963	0.248

Table 4.5 Corals Displaying Vital Effects

name	d47	D47	d48	D48	d13C	d18O	Standard Corrected D47	T	
NT 018	15.63132	0.186437	58.88185	25.51586	-4.63575	41.51038	0.74681058	4.704097	
NT 018	15.39448	0.192188	58.27079	25.1616	-4.761	41.38975	0.75973821	2.391137	
NT 018	15.16933	0.223778	73.07797	39.87223	-4.82713	41.21638	0.7615392	2.073473	
NT 018	15.34129	0.221621	72.94356	39.70716	-4.667	41.2335	0.75389262	3.429828	
NT 018	12.59185	0.129974	66.20617	34.38449	-6.763	40.63038	0.73824471	6.269145	displays Vital Effect
NT 012	12.66207	0.137344	56.60584	24.2974	-7.12375	41.08388	0.81723665	-7.23873	
NT 012	11.92694	0.102082	55.43887	23.41951	-7.70725	40.95638	0.79510827	-3.65345	
NT 012	13.61496	0.172114	58.47579	25.41241	-6.52925	41.36725	0.78184756	-1.43417	
NT 012	13.85587	0.150584	58.27658	25.03667	-6.35525	41.45988	0.75010847	4.108521	
NT 012	13.74895	0.146518	58.35912	25.16717	-6.434	41.43425	0.74804622	4.480499	
NT 012	9.352701	-0.02395	48.09286	18.67026	-8.9515	39.68463	0.70293999	13.01053	displays Vital Effect
NT 012	10.08594	-0.08848	40.20823	10.34648	-8.51925	40.05425	0.72337957	9.049046	displays Vital Effect
NT 012	9.6742	-0.11327	39.8487	10.23738	-8.7895	39.93113	0.69994756	13.60462	displays Vital Effect
NT 012	9.746315	-0.093	40.21668	10.55068	-8.75975	39.95375	0.72230748	9.252759	displays Vital Effect
NT 012	9.603088	-0.09199	40.00354	10.51414	-8.81825	39.86613	0.72519396	8.70529	displays Vital Effect
NT 012	9.973165	0.032681	65.2537	34.9888	-8.55913	39.865	0.71240277	11.1559	displays Vital Effect
NT 012	9.751269	-0.0214	46.01635	16.34367	-8.7065	39.84213	0.70228525	13.1402	displays Vital Effect
NT 012	9.523557	-0.00371	46.02221	16.54354	-8.85688	39.74313	0.72681455	8.39931	displays Vital Effect
NT 014	14.15176	0.173341	60.82013	26.44655	-6.61838	41.99563	0.76945394	0.690359	
NT 014	14.11915	0.161277	60.42125	26.08135	-6.6285	41.985	0.75599303	3.055259	
NT 014	13.75872	0.139085	59.3339	25.41925	-6.70613	41.82188	0.73898241	6.13332	
NT 014	13.57255	0.143543	52.41274	18.96659	-6.82938	41.67088	0.79913414	-4.31653	
NT 014	13.14066	0.178453	72.75109	39.15385	-7.0545	41.42275	0.77437003	-0.15831	
NT 014	13.6076	0.192435	73.13108	39.01066	-6.85188	41.67875	0.77529744	-0.31753	
NT 014	13.30258	0.147566	73.44214	39.63194	-6.9545	41.5185	0.73562198	6.753651	
NT 014	13.28895	0.147076	71.86689	38.20698	-6.91663	41.468	0.73550516	6.77529	
NT 014	9.64182	-0.00433	46.99558	17.34848	-8.80838	39.81488	0.72350563	9.025123	displays Vital Effect
NT 014	13.34258	0.151188	51.61309	18.41459	-6.95675	41.55725	0.81265527	-6.5082	

Table 4.6-14C Dates

UCIAMS	Sample Name	Fm	±	D14C	±	14C age	±
94283	14C-NT-002	0.246821	0.000797	-753.179	0.796519	11240	30
94294	14C-NT-006	0.159514	0.000746	-840.486	0.745506	14745	40
94295	14C-NT-007	0.16904	0.000713	-830.96	0.712631	14280	35
94297	14C-NT-010	0.246049	0.000752	-753.951	0.752397	11265	25
94298	14C-NT-012	0.169699	0.000712	-830.301	0.712215	14250	35
94299	14C-NT-013	0.171814	0.000777	-828.186	0.777304	14150	40
94300	14C-NT-014	0.169222	0.000761	-830.778	0.761363	14270	40
94301	14C-NT-015	0.165354	0.000751	-834.646	0.750784	14455	40
94302	14C-NT-016	0.167163	0.000726	-832.837	0.726462	14370	35
94303	14C-NT-017	0.269392	0.000946	-730.608	0.946269	10535	30
94304	14C-NT-018	0.255347	0.0008	-744.653	0.799811	10965	30
94306	14C-NT-020	0.244856	0.000785	-755.144	0.785297	11305	30
94307	14C-NT-030	0.254247	0.000806	-745.753	0.805702	11000	30
94308	14C-NT-031	0.20836	0.000784	-791.64	0.783763	12600	35
94309	14C-NT-032.	0.179448	0.000793	-820.552	0.793096	13800	40

Table 4.7-U-Series Age determination for Corals

ID	U238 conc ppb	Error	232 Th pmol/g	Error	d234U(T)	Error	230Th/238U	Corrected Age	Error	d234U initial
U-NT002	3396.39	0.64	1.31	0.57	142.90	0.45	0.12	12244	42	147.9336
U-NT006	3569.01	0.84	5.98	0.73	148.35	0.55	0.17	17739	178	155.9805
U-NT007	3448.81	0.84	3.30	0.75	146.65	0.46	0.15	15638	102	153.2785
U-NT010	3072.02	0.90	0.22	0.89	143.94	0.45	0.12	12104	10	148.949
U-NT012	3588.71	0.58	3.79	0.46	145.59	0.45	0.15	15487	113	152.1037
U-NT013	3542.14	0.91	17.39	0.81	146.23	0.39	0.16	15560	527	152.8013
U-NT014	3512.94	0.72	8.85	0.63	144.90	0.41	0.16	16107	270	151.6499
U-NT015	4724.64	1.00	5.12	0.00	139.34	0.40	0.17	17228	116	146.2889
U-NT016	5287.18	4.20	3.93	0.03	142.14	0.45	0.15	15154	80	148.363
U-NT017	3907.84	7.29	25.66	0.09	145.24	0.81	0.12	11773	708	150.1589
U-NT018	5149.60	5.09	20.13	0.04	143.77	0.54	0.14	13870	420	149.5148
U-NT020	4463.25	3.56	4.69	0.03	142.91	0.52	0.12	12168	113	147.9122
U-NT030	3611.69	4.59	23.60	0.06	143.61	0.65	0.12	11889	705	148.5139
U-NT031	3482.02	4.31	2.55	0.05	155.06	0.68	0.16	15698	78	162.0975
U-NT-032	4075.44	3.01	6.79	0.03	147.30	0.45	0.15	15495	178	153.8901

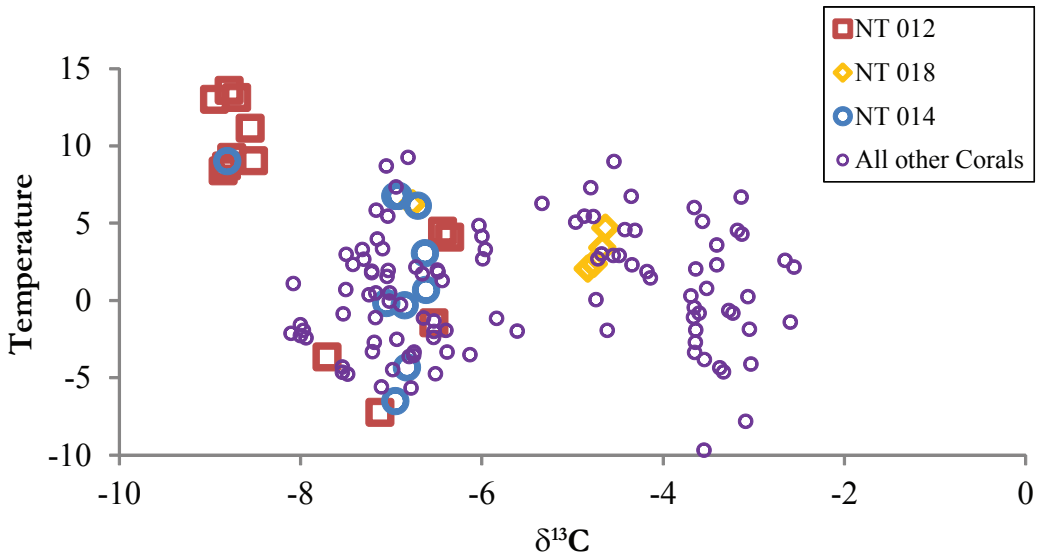

Figure 4.4: Three deep-sea corals exhibit vital effects. This vital effect is exhibited as an increase in temperature that corresponds to very depleted $\delta^{13}C$ values.

very depleted $\delta^{13}C$ values correspond to elevated temperatures. These very depleted $\delta^{13}C$ values are typically found in the centers of calcification (COCs). Future work will involve measuring the clumped isotope value of COCs.

After excluding points, that were effected by vital effects, we reconstructed temperature profiles. The temperature profile for the YD and H1 is much cooler than the modern ocean. The Younger Dryas temperature profile is isothermal -1.5 to 0.5°C at all measured depths. The coral from the Bolling Allerod is as warm as modern at 3.1°C at 1316 m while the H1 profile is isothermal from 1000–2000 m, with a range of (-1.2–-0.2°C). At deeper depths, there is a slight warming to 3.5°C. From 16.1–17.7ka BP at 1427–2459 m the temperature ranges form -1.1–1.3°C implying that the warming at deeper depths started after 16.1 ka BP.

The isothermal temperature profile of the YD and slight warming at deeper depths in the H1 profile implies that the deglacial ocean was stratified by salt as opposed to by temperature as it is in the modern ocean. The $\Delta^{14}C$ profile for the YD ranges from 64-119‰ while the H1 profile ranges from 45–170‰. During late H1, at 1381–2265 m the profile is near constant while below at 2593 m, the $\Delta^{14}C$ is depleted relative to the upper water column.

4.4 DISCUSSION

The corals dated to later in H1 can either be interpreted in two ways; as a time series with four corals at 15.6 ka and one at 15.1 ka, or a single profile of five corals with overlapping 2σ error bars at 15.35 ka. In the first scenario, the 15.6ka profile is isothermal from 1176–2027 m at -0.7°C and there is a slight warming from 2027–2372m of -1.2±1.2°C to 1.6±1°C. At 15.1±0.2 ka, the deep ocean warms to 3.5°C. In the second instance, the profile at 15.35 ka is isothermal between 1381–2027m and exhibits warming with depth.

The increase in temperature at depths in the H1 profile is an unusual feature. This warming at depth implies that salt is controlling the density stratification with depth as

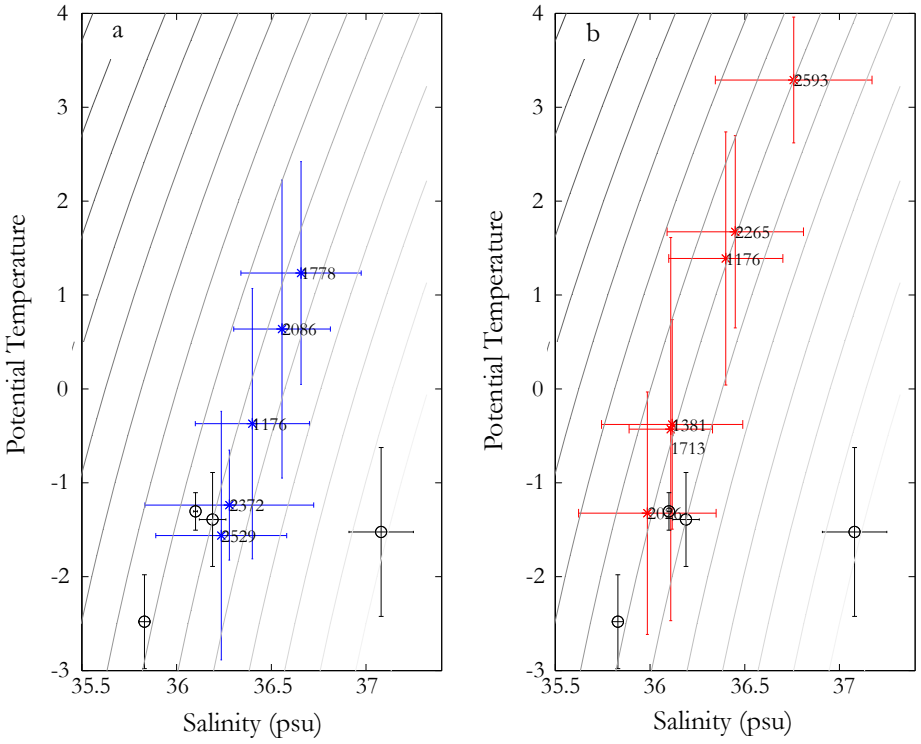

Figure 4.5: The salinity values needed if a constant potential density profile is assumed. (A) LGM theta and salinity estimates in black with the YD in blue. (B) LGM theta and salinity estimates in black with H1 in red. The depths of corals are indicated next to each point.

opposed to temperature, as in the modern ocean. The increase in temperature is a feature of late H1, and begins after 17.1 ka. The warming is also not present during the time of the Younger Dryas seven thousand years later.

Salt stratification in the ocean has been shown to exist during the last glacial time period (18). If we assume constant potential density through the water column we can calculate the minimum salt difference needed to support the warming with depth. We find that the salinity ranges from 36.15 psu to 36.94 psu at late H1 (Figure 4.5), which is within the bounds of the endmembers of the glacial ocean (North Atlantic: 35.83 psu and Southern Ocean: 37.08 psu) (19). This scenario of a salty, warm, and depleted in $\Delta^{14}C$ water below cooler, fresher and more ventilated intermediate waters is consistent with the "thermobaric effect" hypothesis (20).

In the presence of a salt stratified deep ocean, warming at depth can maintain the static stability of the water column. Geothermal heating at the ocean's bottom ranges from 50–100 mW/m^2 (21). For a geothermal heat flux of 50 mW/m^2, 10,000 years are necessary to heat a two km thick parcel of seawater with a salinity difference of 0.4 psu, by 2°C. This long time scale implies that the warming seen at depth at 15.1±0.2 ka must also have been present at 15.6 ka. However if the relevant water mass was thinner, then less time would be required to heat the deeper isopycnals.

The thermobaric effect is a potential energy storage mechanism, a capacitor, which can result in an abrupt overturning of the water column (or deep ocean mixing). As this scenario occurs, the water column changes from having cold fresh water above cold salty water (as in the LGM state) to cold fresh water above warm salty water as geothermal heating occurs. Afterwards cooler waters from the surface are pushed deeper so the water column changes to cold fresh water above warm salty water, above a growing cold water mass. Finally as the density difference between the cold water being pushed downwards and the bottom water mass becomes close to zero, the water column becomes unstable and convects. This convection results in warm salty water above cold fresh water (as in the

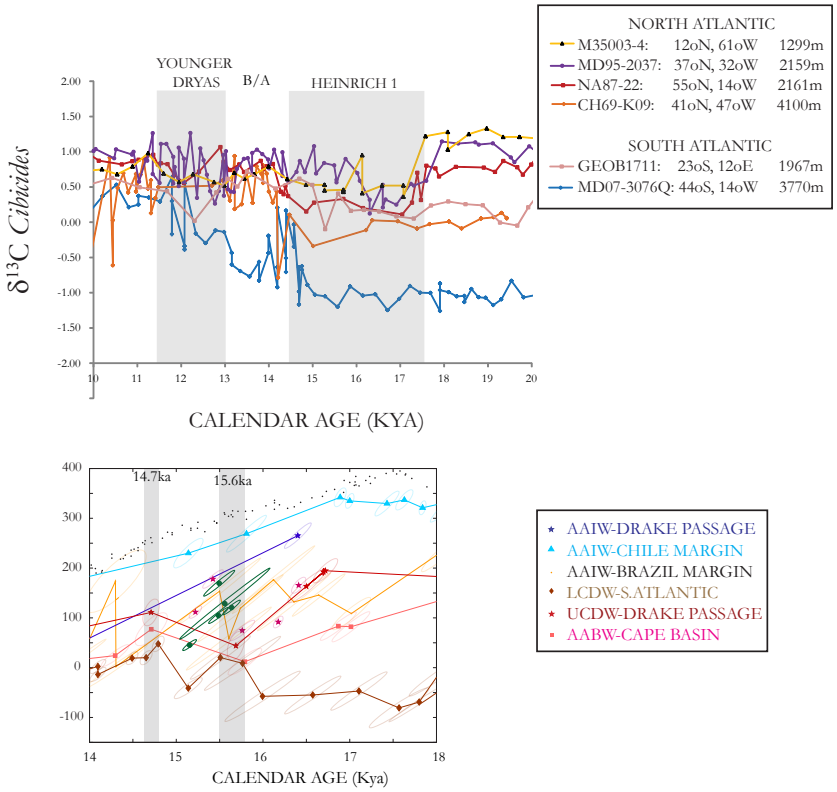

Figure 4.6: (A) The cores that mixed at the end of Heinrich 1 in the North and South Atlantic are all 1200-4100 m. Deeper and shallower cores did not mix. (B) The cores that mixed during at 15.6 ka event in the Southern Ocean are all from deeper isopycnals, while the shallow isopycnals (AAIW by Chile and the corals) did not mix. One core at the Brazilian margin is at a shallower isopycnal and did mix. One possible explanation is the $\Delta^{14}C$ values from the core are affected by methane hydrate seeps.

modern state).

The source of heating at depth could be geothermal heating, but another possibility is a temperature increase at the location of outcropping of the deeper isopycnals, possibly through frontal movement. The "charging of the capacitor" is also seen in the Iberian Margin (22). Similarly to our record, from 17 ka to 15 ka, the deep ocean temperature (as record in Mg/Ca of *G. affinis*) increases from -0.5°C to 2°C (at 3146 m). After which the temperature begins to decline.

The "discharging of the capacitor" is also seen in several other marine and atmospheric records. Benthic $\delta^{13}C$ from the North and South Atlantic show vertical convection of the water column from 1200–4000 m at the beginning of the B/A as the benthic $\delta^{13}C$ at these locations all share a common value of 0.5‰ (Figure 4.6a). This event is also seen in the $\Delta^{14}C$ record as a decrease in ventilation age in the deep South Atlantic and a deepening of the Atlantic overturning circulation (23, 24). The beginning of the Bolling-Allerod is at 14.7 ka is also associated with abrupt changes in the atmosphere (Figure 4.1) (25). There was a sharp rise in pCO_2 of 12 ppmv that lasted 300 years (26) which was also synchronous with the start of the Antarctic Cold Reversal (27) as well as abrupt rises in $\delta^{18}O$ of ice (28). There is also a change in the slope of the $\delta^{13}C_{atm}$ record, as well as a rapid rise in sea level (MWP 1a) (29) and a retreat of sea ice in the Northern Hemisphere (30). These features are all consistent with ocean mixing causing the restart of the AMOC and ventilating an isolated reservoir of carbon causing warming.

There is evidence for two other mixing events occurring over the course of the last glacial termination, at 17.5 and 15.6 ka. At 17.5 ka there are two purported areas of the ocean where increased mixing released CO_2 into the atmosphere, the Southern Ocean and North Pacific. The Southern Ocean shows an increase in upwelling as seen in opal flux (9) and a decline in ^{14}C ages of benthic foraminifera in intermediate depth waters(37). It is thought that this increase in upwelling could have ventilated a deep ocean reservoir near Antarctica which would have supplied ^{14}C-depleted carbon to the atmosphere, causing

the drop in $\Delta^{14}C_{atm}$ that is seen at the start of 17.5 ka. The intermediate depth waters saw this depleted-^{14}C as it was being ventilated to the atmosphere. 17.5 ka is also the time of increased vertical deep convection in the North Pacific which has been shown through a model to have been capable of releasing depleted $\delta^{13}C$ and $\Delta^{14}C$ carbon into the atmosphere (38).

At 15.6 ka, the Southern Ocean's $\Delta^{14}C$ of Upper Circumpolar Deep Water (UCDW), Lower Circumpolar Deep Water (LCDW) and AABW become more similar as the $\Delta^{14}C$ of UCDW and AABW decrease and that of LCDW increases (Figure 4.6b). There is also an intensification of upwelling in the Southern Ocean (9). These changes are indicative of increased deep mixing in the Southern Ocean and a breakdown of the deep vertical stratification that characterizes the LGM. This increased mixing supports the release of carbon from the Southern Ocean and is reflected in changes in slope in the pCO_2, $\Delta^{14}C_{atm}$ and the $\delta^{13}C_{atm}$ records. At essentially the same time (15.4 ka) in the deep North Atlantic there is evidence of increased lateral mixing as seen in older $\Delta^{14}C$ and Cd in a narrow depth range of 1500–2000 m, implying an increase in southern sourced waters (43). This lateral mixing is consistent with the near constant $\Delta^{14}C$ and temperature values seen in the H1 profile between 1300–2000 m. However the effect on the atmospheric record is different than the onset of the termination. There is no change in slope of the pCO_2 record at 15.6, although there is a pause in the decline of $\Delta^{14}C_{atm}$ and an increase in $\delta^{13}C_{atm}$.

The marine benthic $\delta^{13}C$ records do not show a similar mixing pattern as seen in the $\Delta^{14}C$ records. Only the intermediate depth water benthic $\delta^{13}C$ records converge to a single value (implying mixing). The benthic $\delta^{13}C$ records of the shallow depths compared to deeper depths in the North and South Atlantic remain stratified and do not converge until the start of the Bolling/Allerod. Further evidence of this mismatch in timing is seen in a southern Atlantic core, MD07-3076Q at 44° S, 14° W and 3770 m which shows the mixing in $\Delta^{14}C$ (41) occurring at a deeper depth in the core than the increase in $\delta^{13}C$ to a heavier value of 0.5‰ (22).

One explanation for this seeming discrepancy is as follows. At 15.6 ka, the Southern Ocean begins to mix vertically which is exhibited in $\Delta^{14}C$ records from the Southern Ocean. This mixing is seen in $\Delta^{14}C$ because the different water masses have dramatically different $\Delta^{14}C$ values, so any change in mixing is seen rapidly in $\Delta^{14}C$. $\delta^{13}C$ in ocean is a nonconservative tracer, so this mixing might have coincided with changes in air-sea gas exchange or remineralization rates which masked the mixing event in $\delta^{13}C$. This mixing event must also have been associated with an increase in formation of southern sourced intermediate waters, or a decrease in formation of Glacial North Atlantic Intermediate waters. This change allows southern sourced waters to arrive in the North Atlantic and cause lateral mixing there, as seen in high Cd, and depleted $\Delta^{14}C$ (42, 43). At the start of the Bolling-Allerod, at 14.7 ka, there is the restart of the AMOC and increased warming. This restart of AMOC brings NADW (high in $\delta^{13}C$) to the deep North and South Atlantic explaining the mixing seen in $\delta^{13}C$ and $\Delta^{14}C$. The warm coral at 15.1 ka could show evidence of geothermal heating warming the bottom before destabilizing the water column allowing for AMOC to resume.

An alternate explanation for the warming at depth in the late H1 profile, which does not involve the "Thermobaric Capacitor Hypothesis", is perhaps that the NW Atlantic is seeing the warming of a deep water mass. The deeper points in the profile could reflect a depleted warm Southern sourced deep water in the North Atlantic while the depths between 1300–2000 m could reflect the presence of a ventilated cool Northern sourced water. There is evidence for deglacial warming of the surface ocean in high Southern latitudes (44, 45). This warming could be transferred to depth by deep water formation and thus be reflected in our profile.

The Younger Dryas profile at 12.1–11.7 ka occurs at a time when the state of the ocean during the YD/Holocene transition was very different to the deglacial ocean during H1. Deep water formation had slowed allowing fresh water to pool on the surface as the result of extensive winter sea ice cover (30). This shut down of AMOC led to a cooling

of the Northern hemisphere which caused a southward shift to the ITCZ (11) as well as a weakened Asian Monsoon (6). The atmospheric records also show strong changes., for instance the CO_2 record begins to rise at the YD after stalling at the Bolling Allerod. This rise is associated with a burst of upwelling in the Southern Ocean(9). At the start of the YD, the $\Delta^{14}C_{atm}$ initially rises, which is thought to be associated with the reduction of $\Delta^{14}C$ oceanic exchange due to the slowdown of AMOC that persisted for ~ 200 years. At 12.6 ka, the $\Delta^{14}C_{atm}$, declines which is consistent with a reinvigoration of NADW or the activation of another radiocarbon sink which brings radiocarbon back into equilibrium with the atmosphere.

At the start of the YD, the $\delta^{13}C$ of *Cibicides* in the deep North and South Atlantic (41), and Cd/Ca ratios indicate an increased Southern influence to deep North Atlantic, while the intermediate depth records are more equivocal and indicate either an increased Southern (42) or Northern influence (46). At 12.2 ka (within error of the beginning of the decline of $\Delta^{14}C_{atm}$ and the beginning of Southern Ocean upwelling) the $\delta^{13}C$ of Cibicides in the North Atlantic from 1200–4100 m and the deep South Atlantic approach 0.57‰, implying mixing within those isopycnals. This is also a time of increased upwelling in the Southern Ocean(9). Later at 11.6 ka in the intermediate depth waters in the NW Atlantic there are very large and mobile gradients in $\Delta^{14}C$ (47). Our temperature and $\Delta^{14}C$ record at 12.1–11.7 ka are nearly constant with depth and occur after the mixing event in the North and South Atlantic and likely before the appearance of transients in the intermediate depth waters. However future work of top, middle and bottom radiocarbon dates will elucidate the exact timing of our profile relative to the appearance of transients.

4.5 CONCLUSIONS

In conclusion, we show coupled radiocarbon, U-series and clumped isotope measurements that show evidence for salinity stratification at late H1 and the YD. We also find increased warming at depth during late H1 which could be consistent with the charging of a "Thermobaric Capacitor" at the beginning of the B/A. The discharge of

the capacitor causes the ocean to convect and release CO_2 into the atmosphere, which is seen in marine benthic $\delta^{13}C$, $\Delta^{14}C$ and atmospheric records. We review other oceanic mixing events that occurred during the termination and find they each had a different signature in marine and atmospheric records. The 17.8 ka event released CO_2 into the atmosphere and initiated warming while shutting down AMOC. The 15.6 ka event did also change the slope of the pCO_2 record and $\delta^{13}C$ record, and the benthic $\Delta^{14}C$ record but not $\delta^{13}C$ record. We also place the YD in the context of other marine records and conclude that our record takes place after an oceanic mixing event that released CO_2 into the atmosphere. This is supported by the nearly constant temperature and $\Delta^{14}C$ seen in the profile.

References

1. EPICA, Eight glacial cycles from an Antarctic ice core. Nature 429, 623 (2004).

2. W. Dansgaard et al., North Atlantic climate oscillations revealed by deep Greenland Cores, Climate Processes and Climate Sensitivity. Am. Geophy. Union Mon. 29, 288 (1984).

3. C. D. Charles, J. Lynch-Stieglitz, U. S. Ninnemann, R. G. Fairbanks, Climate connections between the hemisphere revealed by deep sea sediment core/ice core correlations. Earth Planet Sc Lett 142, 19 (1996).

4. R. J. Behl, J. P. Kennett, Brief interstadial events in the Santa Barbara basin, NE Pacific, during the past 60 kyr. Nature 379, 243 (1996).

5. X. Wang et al., Wet periods in northeastern Brazil over the past 210 kyr linked to distant climate anomalies. Nature 432, 740 (2004).

6. Y. J. Wang et al., A high-resolution absolute-dated late Pleistocene monsson record from Hulu Cave, China. Science 294, 2345 (2001).

7. T. Blunier, E. Brook, Timing of millennial-scale climate change in Antarctica and Greenland during the last glacial period. Science 291, 109 (2001).

8. B. Lemieux-Dudon et al., Consistent dating for Antarctic and Greenland ice cores. Quaternary Sci Rev 29, 8 (2010).

9. R. F. Anderson et al., Wind-Driven Upwelling in the Southern Ocean and the Deglacial Rise in Atmospheric CO2. Science 323, 1443 (March 13, 2009, 2009).

10. J. C. H. Chiang, C. M. Bitz, Influence of high latitude ice cover on the marine intertropical convergence zone. Clim Dynam 25, 477 (2005).

11. J. C. H. Chiang, The Tropics in Paleoclimate. Annual Review of Earth and Planetary Sciences 37, 263 (2009/05/01, 2009).

12. J. F. Adkins, A. P. Ingersoll, C. Pasquero, Rapid climate change and conditional instability of the glacial deep ocean fron the thermobaric effect and geothermal heating. Quaternary Sci Rev 24, 581 (2005).

13. J. F. Adkins, K. McIntyre, D. P. Schrag, The salinity, temperature, and delta O-18 of

the glacial deep ocean. Science 298, 1769 (Nov 29, 2002).

14. J. F. Adkins et al., Radiocarbon dating of deep-sea corals. Radiocarbon 44, 567 (2002).

15. L. F. Robinson et al., Deep-sea scleractinian coral age and depth distributions in the NW Atlantic for the last 225 thousand years. B Mar Sci 81, 371 (2007).

16. N. G. Thiagarajan, D. S.; Roberts, M.; McNichol, A. P.; Thresher, R.; Adkins, J. F., paper presented at the American Geophysical Union, San Francisco, 2009.

17. A. Burke et al., Reconnaissance dating: A new radiocarbon method applied to assessing the temporal distribution of Southern Ocean deep-sea corals. Deep Sea Research Part I: Oceanographic Research Papers 57, 1510 (2010).

18. J. F. Adkins, K. McIntyre, D. P. Schrag, The salinity, temperature, and d18O of the glacial deep ocean. Science 298, 1769 (2002).

19. J. F. Adkins, K. McIntyre, D. P. Schrag, The temperature, salinity and delta O-18 of the LGM deep ocean. Geochim Cosmochim Ac 66, A7 (Aug, 2002).

20. J. F. Adkins, A. P. Ingersoll, C. Pasquero, Rapid climate change and conditional instability of the glacial deep ocean from the thermobaric effect and geothermal heating. Quaternary Sci Rev 24, 581 (Mar, 2005).

21. C. A. Stein, S. Stein, A model for the global variation in oceanic depth and heat-flow with lithospheric age. Nature 359, 123 (1992).

22. L. C. Skinner, N. J. Shackleton, Deconstructing Terminations I and II: revisiting the glacioeustatic paradigm based on deep-water temperature estimates. Quaternary Sci Rev 25, 3312 (2006).

23. S. Barker, G. Knorr, M. J. Vautravers, P. Diz, L. C. Skinner, Extreme deepening of the Atlantic overturning circulation during deglaciation. Nature Geosci 3, 567 (2010).

24. J. McManus, R. Francois, J. Gherardi, L. Keigwin, S. Brown-Leger, Collapse and rapid resumption of Atlantic meridional circulation linked to deglacial climate changes. Nature 428, 834 (2004).

25. J. P. Steffensen et al., High-Resolution Greenland Ice Core Data Show Abrupt Climate Change Happens in Few Years. Science 321, 680 (August 1, 2008, 2008).

26. A. Lourantou, J. Chappellaz, J. M. Barnola, V. Masson-Delmotte, D. Raynaud, Changes in atmospheric CO2 and its carbon isotopic ratio during the penultimate deglaciation. Quaternary Sci Rev 29, 1983 (2010).

27. B. Stenni et al., An Oceanic Cold Reversal During the Last Deglaciation. Science 293, 2074 (September 14, 2001, 2001).

28. NGRIP, High-resolution record of Northern Hemisphere climate extending into the last interglacial period. Nature, 147 (2004).

29. A. J. Weaver, O. A. Saenko, P. U. Clark, J. X. Mitrovica, Meltwater Pulse 1A from Antarctica as a Trigger of the Bølling-Allerød Warm Interval. Science 299, 1709 (March 14, 2003, 2003).

30. G. H. Denton, R. B. Alley, G. C. Comer, W. S. Broecker, The role of seasonality in abrupt climate change. Quaternary Sci Rev 24, 1159 (2005).

31. EPICA, One-to-one coupling of glacial cliamte variability in Greenland and Antarctica. Nature 444, 195 (2006).

32. J. Southon, A. L. Noronha, H. Cheng, R. L. Edwards, Y. Wang, A high-resolution record of atmospheric 14C based on Hulu Cave speleothem H82. Quaternary Sci Rev 33, 32 (2012).

33. J. Schmitt et al., Carbon Isotope Constraints on the Deglacial CO2 Rise from Ice Cores. Science, (March 29, 2012, 2012).

34. S. R. Hemming, Heinrich events: Massive late Pleistocene detritus layers of the North Atlantic and their global climate imprint. Reviews of Geophysics 42, RG1005 (2004).

35. H. Heinrich, Origin and consequences of cyclic ice rafting in the northeast Atlantic Ocean during the past 130,000 years. Quaternary Research 29, 142 (1988).

36. S. Toucanne et al., Timing of massive 'Fleuve Manche' discharges over the last 350 kyr: insights into the European ice-sheet oscillations and the European drainage

network from MIS 10 to 2. Quaternary Sci Rev 28, 1238 (2009).

37. T. M. Marchitto, S. Lehman, J. Ortiz, J. Fluckiger, A. vanGeen, Marine radiocarbon evidence for the Mechanism of deglacial atmospheric CO2 rise. Science 316, 1456 (2007).

38. J. Rae, Foster, G, Gutjahr, M, Sarnthein, M, Skinner, L, Schmidt, D, Elliot, T paper presented at the Goldschmidt, Prague, 2011.

39. C. Laj et al., Geomgnetic field intensity, North Atlantic deep water circulation and atmospheric D14C during the last 50 kyr. Earth Planet Sc Lett 200, 177 (2002).

40. R. Muscheler et al., Changes in the carbon cycle during the last deglaciation as indicated by the comparison of 10Be and 14C records. Earth Planet Sc Lett 219, 325 (2004).

41. C. Waelbroeck et al., The timing of deglacial circulation changes in the Atlantic. Paleoceanography 26, PA3213 (2011).

42. R. E. M. Rickaby, H. Elderfield, Evidence from the high-latitude North Atlantic for variations in Antarctic Intermediate water flow during the last deglaciation. Geochem Geophy Geosy 6, doi:1029/2004GC000858 (2005).

43. J. F. Adkins, H. Cheng, E. A. Boyle, E. R. M. Druffel, L. Edwards, Deep-sea coral evidence for rapid change in ventilation of the deep North Atlantic 15,400 years ago. Science 280, 725 (1998).

44. E. Calvo, C. Pelejero, P. De Deckker, G. A. Logan, Antarctic deglacial pattern in a 30 kyr record of sea surface temperature offshore South Australia. Geophys. Res. Lett. 34, L13707 (2007).

45. F. Lamy et al., Antarctic Timing of Surface Water Changes off Chile and Patagonian Ice Sheet Response. Science 304, 1959 (June 25, 2004, 2004).

46. T. M. Marchitto, W. B. Curry, D. W. Oppo, Millennial-scale changes in North Atlantic circulation since the last glaciation. Nature 393, 557 (1998).

47. S. F. Eltgroth, J. F. Adkins, L. F. Robinson, J. Southon, M. Kashgarian, A deep-sea coral record of North Atlantic radiocarbon through the Younger Dryas: Evidence for intermediate water/deepwater reorganization. Paleoceanography 21, (Nov 17, 2006).